University of Kent

Kent Academic Repository

Souza, Cauê P and Fantuzzi, Felipe (2024) *Computational strategies for modelling excited states in organometallic chemistry*. In: Bakewell, Clare and Costa, Nildo and Musgrave, Rebecca and Owen, Gareth, eds. Organometallic Chemistry. Specialist Periodical Reports (SPR) - Organometallic Chemistry . Royal Society of Chemistry, pp. 271-316. ISBN 978-1-83767-461-9.

Downloaded from
https://kar.kent.ac.uk/108554/ The University of Kent's Academic Repository KAR

The version of record is available from
https://doi.org/10.1039/9781837676200

This document version
Publisher pdf

DOI for this version

Licence for this version
CC BY-NC-ND (Attribution-NonCommercial-NoDerivatives)

Additional information

Versions of research works

Versions of Record
If this version is the version of record, it is the same as the published version available on the publisher's web site. Cite as the published version.

Author Accepted Manuscripts
If this document is identified as the Author Accepted Manuscript it is the version after peer review but before type setting, copy editing or publisher branding. Cite as Surname, Initial. (Year) 'Title of article'. To be published in ***Title of Journal*** , Volume and issue numbers [peer-reviewed accepted version]. Available at: DOI or URL (Accessed: date).

Enquiries
If you have questions about this document contact ResearchSupport@kent.ac.uk. Please include the URL of the record in KAR. If you believe that your, or a third party's rights have been compromised through this document please see our Take Down policy (available from https://www.kent.ac.uk/guides/kar-the-kent-academic-repository#policies).

Computational strategies for modelling excited states in organometallic chemistry[†]

Cauê P. Souza and Felipe Fantuzzi*

DOI: 10.1039/9781837676200-00271

This chapter explores advanced computational methods and strategies to model excited states in organometallic systems, essential for advancing discovery, design, and comprehension in fields such as photocatalysis, artificial photosynthesis, and light-responsive materials. We initiate with a fundamental discussion on available quantum mechanical approaches for organometallic compounds, stressing the importance of carefully choosing theoretical methods that are specifically suited to their unique characteristics. We delineate the theoretical underpinnings and practical applications of various electronic structure methods, including density functional theory (DFT) and post-Hartree–Fock approaches, and detail their adaptability to the unique properties of transition metal complexes. Particular attention is given to multireference and perturbative methods, which are critical for accurately describing the complex electronic structure typical of organometallic compounds. Through hierarchical classification, critical evaluation, and carefully curated references, this chapter serves as both a primer and a deep dive into the computational toolbox available for organometallic researchers, offering insights into method selection and application challenges.

1 Electronic structure methods

Recent decades have seen the emergence of a plethora of quantum mechanical methods to simulate and predict the properties and energies of excited states, with applications extending across a variety of chemical systems. To the untrained eye, such diversity might give the impression that any particular problem can be solved equally in many ways. However, navigating judiciously this complex array of methods requires an understanding of the theoretical basis and capabilities of each method in order to critically assess their suitability for the problem at hand. One must be able to tell alpacas from llamas, and this is not done by their hums.

In this chapter, we aim to cover the most significant aspects of electronic structure levels of theory (Section 1) and accompanying excited state methods (Section 2), offering a hierarchical classification whenever possible. Applications and current practical achievements in the context of excited state calculations of organometallic systems are discussed in Section 3. Careful attention is given to the approximations made and their impact on accuracy when treating organometallics. In doing so, we avoid diving into extensive mathematical formalism, but appropriate references are provided for interested readers. This chapter, therefore, serves as an introductory

School of Chemistry and Forensic Science, University of Kent, Park Wood Rd, Canterbury CT2 7NH, UK. E-mail: f.fantuzzi@kent.ac.uk

[†] This chapter is subject to a Creative Commons CC-BY-NC-ND 4.0 International license. Financial support from the Engineering and Physical Sciences Research Council (grant no. EP/W52461X/1), the University of Kent, the European Commission (grant no. GA 872494) and European Cooperation in Science and Technology is acknowledged.

© The Royal Society of Chemistry 2024

Downloaded from http://books.rsc.org/books/edited-volume/chapter-pdf/1851664/bk9781837676200-00271.pdf by University of Kent user on 28 January 2025

guide or roadmap to these methodologies. The reason we begin by discussing the various models of electronic structure theory is that all electronic and chemical properties—including excited states—are based on them. Therefore, the accuracy and quality of the computed properties are fundamentally dependent on the chosen models.

1.1 Quantum mechanics and the Schrödinger equation

Quantum mechanics—or more generally, quantum field theory (QFT)—provides us a way of describing physical systems at the subatomic level, in principle, in a complete and exact way, provided we neglect gravitational interactions. This optimistic picture is, however, destroyed in many ways by mathematical or practical impossibilities. This forces us to approximate our model in different, and quite clever, ways. Our treatment of the description of chemical systems here will consider what is currently available as computational resources implemented in standard software packages, thus limiting the scope of this text. We will concentrate on a particle-based theory (*i.e.* ignoring the quantum field picture) which initially neglects any relativistic effects (we will come back to these in Section 1.8). In other words, we will use the Schrödinger equation, and assume the accompanying standard collection of postulates as the foundation of our model.[1] The electronic spin—essentially a relativistic property—will be introduced in an *ad hoc* manner, as it is indispensable for the correct description of atoms and molecules.

The full (or time-dependent) Schrödinger equation (TDSE) can describe temporal and spatial phenomena in a quantum system and is general in the non-relativistic scenario:

$$\mathcal{H}(\boldsymbol{r},\boldsymbol{R},t)\Psi(\boldsymbol{r},\boldsymbol{R},t)=i\hbar\frac{\partial\Psi(\boldsymbol{r},\boldsymbol{R},t)}{\partial t} \tag{1}$$

where $\mathcal{H}(\boldsymbol{r},\boldsymbol{R},t)=T(\boldsymbol{r},\boldsymbol{R})+V(\boldsymbol{r},\boldsymbol{R},t)$ is the Hamiltonian operator composed of the kinetic (T) and potential (V) energies for the system; $\boldsymbol{r}$ and $\boldsymbol{R}$ are the electronic and nuclear spatial coordinates, respectively. Without loss of generality, for a time-independent potential (such as the nuclear potential in atoms and molecules), the wavefunction can be separated into the product of a time-dependent and a time-independent part by separation of variables:

$$\Psi(\boldsymbol{r},\boldsymbol{R},t)=f(t)\psi(\boldsymbol{r},\boldsymbol{R}) \tag{2}$$

leading to the time-independent Schrödinger equation (TISE), and a time-dependent part $f(t)$:

$$\mathcal{H}\psi_i(\boldsymbol{r},\boldsymbol{R})=E_i\psi_i(\boldsymbol{r},\boldsymbol{R}) \tag{3}$$

$$f(t)=\mathrm{e}^{-\frac{i}{\hbar}E_tT} \tag{4}$$

The solution of eqn (3) yields a complete set of electronic state wavefunctions $\{\psi_i\}$ and their respective energies $\{E_i\}$. Each wavefunction contains all possible information about its electronic state and can be used with suitable operators to obtain the expectation values of any observables. However, this picture is complicated even for simple atomic systems containing more than one electron. To understand why, let us consider a

Downloaded from http://books.rsc.org/books/edited-volume/chapter-pdf/1851664/bk9781837676200-00271.pdf by University of Kent user on 28 January 2025

standard non-relativistic Hamiltonian for a system that contains N electrons and M nuclei, and is devoid of external potential interactions:

$$\mathcal{H} = -\frac{1}{2}\sum_{i=1}^{N}\nabla_i^2 - \frac{1}{2}\sum_{A=1}^{M}\frac{1}{M_A}\nabla_A^2 - \sum_{i=1}^{N}\sum_{A=1}^{M}\frac{Z_A}{r_{iA}} + \sum_{i=1}^{N}\sum_{j>i}^{N}\frac{1}{r_{ij}} + \sum_{A=1}^{M}\sum_{B>A}^{M}\frac{Z_A Z_B}{R_{AB}} \tag{5}$$

In eqn (5), M_A is the mass of nucleus A; Z_A is the total charge of nucleus A; r_{iA}, r_{ij}, and R_{AB} are the distances between electron i and nucleus A, electrons i and j, and nuclei A and B, respectively. This Hamiltonian is written in atomic units. The first two terms are the kinetic energy of the electrons and nuclei, respectively; the last three terms describe the Coulomb electron–nucleus interaction, the electron–electron interaction, and the nucleus–nucleus interaction, respectively.

If we consider atomic systems (for which the second and last terms in eqn (5) are void), the TISE has exact analytic solution only for hydrogenic atoms. This is because the pairwise electron–electron interaction is impossible to solve exactly in multi-electronic systems. If we consider molecular systems, an additional complication arises. Because nuclei can also move relative to one another, accounting for the dynamic electron–nucleus interactions becomes complicated. Additionally, another key approximation made in quantum chemical models is the Born–Oppenheimer (BO) approximation. In simplified terms, the BO approximation involves neglecting the coupling of electronic and nuclear dynamics, effectively treating electrons as if they were influenced only by a static field of fixed nuclei. With this approximation, the second term in eqn (5) disappears and the last term is a constant, which contributes only to the energy of the states, and not to their wavefunctions. One can then write the solution of the TISE in the BO approximation as:

$$\mathcal{H}_{\mathrm{el}}\Phi_i(\boldsymbol{r},\boldsymbol{R}) = V_i(\boldsymbol{R})\Phi_i(\boldsymbol{r},\boldsymbol{R}) \tag{6}$$

where $\mathcal{H}_{\mathrm{el}}$ is the electronic Hamiltonian and $V_i(\boldsymbol{R})$ are the energies of the electronic levels Φ_i, which depend *only parametrically* on the nuclear coordinates $\boldsymbol{R}$. This dependency is referred to as the potential energy surface (PES). Since the Hamiltonian is a Hermitian operator, the solutions $\{\Phi_i\}$ constitute a complete basis set, allowing the total wavefunction to be expressed as a linear combination of these basis functions:

$$\psi(\boldsymbol{r},\boldsymbol{R}) = \sum_i C_i(\boldsymbol{R})\Phi_i(\boldsymbol{r},\boldsymbol{R}) \tag{7}$$

The reader interested in a more quantitative and in-depth treatment of the BO approximation may consult ref. 2–5. In this text, we will reserve the upper-case psi (Ψ) for the total time-dependent wavefunction, the lower-case psi (ψ) for the total time-independent wavefunction, the upper-case phi (Φ) for the electronic wavefunctions, and later on, the lower-case phi (ϕ) for spatial orbitals, or one-electron wavefunctions. With this definition, we will omit the Hamiltonian subscript as it becomes superfluous.

Downloaded from http://books.rsc.org/books/edited-volume/chapter-pdf/1851664/bk9781837676200-00271.pdf by University of Kent user on 28 January 2025

1.2 The Hartree–Fock method

Up to this point, we have introduced two approximations to our models: (1) relativistic effects are neglected; (2) the BO approximation is adopted for molecules. The problem of solving the electronic Schrödinger equation for multi-electron systems persists. The most popular approach to this end is the Hartree–Fock (HF) method. It is the basis for a variety of higher quality methods usually classified as post-Hartree–Fock (post-HF) methods. At the heart of the HF approach is the introduction of an *independent particle model* (IPM), in which the instantaneous interactions between electrons are neglected. Instead, each particular electron is subjected to the space- and spin-averaged potential of all other electrons. Each electron is described by a spin–orbital—a product of a spin function and the spatial wavefunction of an electron in a hydrogenic system. Spin–orbitals are typically expressed as a linear combination of atomic basis set functions. Ideally, a complete basis set would include an infinite number of these functions; however, in practice, truncated basis sets must be used. The optimal set of spin–orbitals is obtained through the variational principle, *i.e.* the spin–orbitals for the ground state are those that minimise the energy $E_0 = \langle \Phi_0 | \mathcal{H} | \Phi_0 \rangle$. This minimisation leads to eigenvalue equations of the form:

$$\mathcal{F}(i)|\chi(\boldsymbol{x}_i)\rangle = \epsilon|\chi(\boldsymbol{x}_i)\rangle \tag{8}$$

where $\chi(\boldsymbol{x}_i) = \phi_i(\boldsymbol{r}_i)\alpha(\boldsymbol{\omega}_i)$ or $\chi(\boldsymbol{x}_i) = \phi_i(\boldsymbol{r}_i)\beta(\boldsymbol{\omega}_i)$ is the spin–orbital for electron i, with α and β being the two possible spin functions, and $\mathcal{F}(i)$ is the Fock operator given by:

$$\mathcal{F}(i) = -\frac{1}{2}\nabla_i^2 - \sum_{A=1}^{M}\frac{Z_A}{r_{iA}} + \upsilon^{\mathrm{HF}}(i) = h(i) + \upsilon^{\mathrm{HF}}(i) \tag{9}$$

where $\upsilon^{\mathrm{HF}}(i)$ is the average potential to which electron i is subjected. Since this potential depends on all the orbitals which are solution to the HF equation, it must be solved iteratively using the self-consistent field (SCF) method. In the SCF method, one starts with an initial guess for the orbitals and solves the HF equation to obtain a new set of orbitals. These new orbitals are then utilised to solve the HF equation again. This iterative procedure is repeated until the resulting orbitals converge and are virtually indistinguishable from those of the previous iteration.

The total electronic wavefunction Φ_0 is assembled as a Slater determinant of the optimal electronic spin–orbitals of the system:

$$\Phi_0(\boldsymbol{x}_1, \boldsymbol{x}_2, \ldots, \boldsymbol{x}_N) = (N!)^{\frac{1}{2}}\begin{vmatrix} \chi_i(\boldsymbol{x}_1) & \chi_j(\boldsymbol{x}_1) & \cdots & \chi_k(\boldsymbol{x}_1) \\ \chi_i(\boldsymbol{x}_2) & \chi_j(\boldsymbol{x}_2) & \cdots & \chi_k(\boldsymbol{x}_2) \\ \vdots & \vdots & \ddots & \vdots \\ \chi_i(\boldsymbol{x}_N) & \chi_j(\boldsymbol{x}_N) & \cdots & \chi_k(\boldsymbol{x}_N) \end{vmatrix} \tag{10}$$

This approach guarantees that the wavefunction is antisymmetric with respect to the exchange of any pair of electrons, as required for

Downloaded from http://books.rsc.org/books/edited-volume/chapter-pdf/1851664/bk9781837676200-00271.pdf by University of Kent user on 28 January 2025

indistinguishable fermions. While this condition is necessary for a correct description of the wavefunction, *it is not sufficient on its own*. In fact, a correct wavefunction must also form a basis for the symmetric group S_N (where N is the number of electrons), thereby reflecting the symmetry of the Hamiltonian (more on this in Section 1.6).

Since the HF method models the wavefunction as one Slater determinant, the variational principle optimises the energy subjected to this restriction. Such methods are called single-determinant methods, and the reader is referred to ref. 6 for a detailed description of the HF method.

1.3 Configuration interaction

As we have seen, HF theory only accounts for electron–electron interactions in an averaged fashion. Because the instantaneous effect of the correlated motion of electrons does not exist in this theory, we say it lacks *electronic correlation*. The electronic correlation energy (E_{corr}) of a system is traditionally defined as the difference between its exact non-relativistic energy (ϵ_0) and its (restricted) HF energy in the limit of a complete basis set ($E_{\text{HF/CBS}}$):

$$E_{\text{corr}} = \epsilon_0 - E_{\text{HF/CBS}} \tag{11}$$

Such a definition assumes that the only effect separating the exact non-relativistic energy and the HF energy is electronic correlation effects—an assumption proven wrong (see Section 1.6). It is also common practice to partition E_{corr} into a *static* (or *non-dynamic*) and a *dynamic* part. Static correlation is a denomination to the effect of some systems being only correctly described by a combination of different near-degenerate configurations, which the single-reference HF wavefunction cannot account for. Dynamic correlation is then the effect of the instantaneous correlated movement of the electrons. In Section 1.6 we will briefly discuss the validity of such definitions.

The most straightforward way to introduce electronic correlation in the HF framework is by using configuration interaction (CI) methods. As discussed above, the ground state HF wavefunction is in the form of a single Slater determinant. Such a wavefunction consists of a set of lower energy occupied spin–orbitals and a set of higher energy virtual (*i.e.* unoccupied) spin–orbitals. By exchanging occupied and virtual orbitals in such a determinant, one can construct excited Slater determinants. Note that "excited" here refers to the form of the determinant, not to excited electronic states of the system. If only one such exchange is made, we call it a singles (S) determinant. Analogously, doubles (D), triples (T), quadruples (Q), and so on, determinants can be constructed depending on whether two, three, four, *etc.* exchanges are made, up to the number N of electrons in the system. The size of the basis set utilised to expand the orbitals determines the number of virtual orbitals present in the wavefunction, and thus, the number of possible excited determinants.

The CI method is based on the variational principle. The wavefunction *ansatz* is expressed as a linear combination of Slater

Downloaded from http://books.rsc.org/books/edited-volume/chapter-pdf/1851664/bk9781837676200-00271.pdf by University of Kent user on 28 January 2025

determinants derived from excitations of the reference ground state HF determinant:

$$\Phi_{\mathrm{CI}} = a_0\Phi_{\mathrm{HF}} + \sum_{\mathrm{S}} a_{\mathrm{s}}\Phi_{\mathrm{S}} + \sum_{\mathrm{D}} a_{\mathrm{D}}\Phi_{\mathrm{D}} + \sum_{\mathrm{T}} a_{\mathrm{T}}\Phi_{\mathrm{T}} + \sum_{\mathrm{Q}} a_{\mathrm{Q}}\Phi_{\mathrm{Q}} + \cdots \quad (12)$$

The coefficients of this expansion are determined upon the condition that the energy should be a minimum and the wavefunction be normalised. This leads to the following Lagrange equation:

$$L = \langle\Phi_{\mathrm{CI}}|\mathcal{H}|\Phi_{\mathrm{CI}}\rangle - \lambda(\langle\Phi_{\mathrm{CI}}|\Phi_{\mathrm{CI}}\rangle - 1) \quad (13)$$

We will not attempt to go further in the solutions of this problem, which are well described in ref. 6 and 7. For an infinite basis set, considering all possible excited Slater determinants (a complete basis for the wavefunction expansion) would yield the exact solution of the electronic Schrödinger equation within the non-relativistic and BO approximation frameworks. The result of a CI calculation is a series of eigenvalues and eigenfunctions, which can be viewed as the outcome of diagonalising the CI matrix. The smallest eigenvalue is the ground state energy, with its corresponding eigenfunction being the ground state wavefunction. The second lowest eigenvalue and its associated wavefunction correspond to the first excited state, and so on.

One can easily perceive that a full CI calculation is unfeasible but for the smallest systems. In fact, given $2K$ spin–orbitals for a system of N electrons, there are $\binom{2K}{N}$ possible Slater determinants. This notation represents the number of ways to choose N spin–orbitals out of $2K$ without considering the order. Essentially, it calculates how many different ways we can arrange N electrons into $2K$ available spin–orbitals. As both N and $2K$ increase, the number of possible configurations increases rapidly, in a combinatorial explosion.

A common approximation for chemical purposes is to consider only the excited determinants arising from valence electrons, known as the *frozen core* approximation. The absolute error of introducing such a procedure is not small. However, since core electrons respond weakly to chemical changes, this leads to good relative energies due to error cancelation.

In addition to the *frozen core* approximation, CI calculations are typically performed using a truncated expansion, which limits the inclusion of excited determinants based on their order. Including only single excitations (CIS) does not improve the HF wavefunction because integrals involving singly excited determinants and the HF reference are zero because of orthogonality. Thus, the smallest improvement can be achieved by considering doubly excited determinants, either alone (CID) or with singles (CISD). The latter offers a slight improvement because the overlap between singles and doubles is non-zero.

Further improvements can be made by including triply (CISDT) and quadruply (CISDTQ) excited determinants. The latter often approaches sufficiently close the full CI energy for many systems, but it becomes extremely costly for large molecules and basis sets. While singly excited determinants contribute minimally to the electronic energy of a system,

Downloaded from http://books.rsc.org/books/edited-volume/chapter-pdf/1851664/bk9781837676200-00271.pdf by University of Kent user on 28 January 2025

they are crucial for calculating molecular properties, such as the ones we will consider in Section 2.

In the CI method described above, the spin–orbitals composing each Φ_i Slater determinant are those obtained as solutions to the HF equations. Further variational freedom can be introduced to the various truncated CI methods by allowing the coefficients of each orbital expansion in the basis set to be optimised variationally alongside the CI coefficients. This approach, known as the *multiconfiguration self-consistent-field* (MCSCF) method, is clearly more expensive than standard CI methods, but the wavefunction converges better and faster to the variational limit.

An MCSCF wavefunction can more accurately describe systems that require different electronic configurations for a balanced representation, such as organometallic molecules with heavier metals, where spin–orbit coupling mixes different spin configurations into the electronic states. In essence, MCSCF methods are multideterminant, as they do not rely on a single HF determinant as the reference for excited determinants in the expansion.

One challenge with MCSCF methods is the selection of appropriate configurations to include in the calculations. A frequently used approach is the *complete active space self-consistent-field* (CASSCF) method, which partitions the molecular orbitals into active and inactive spaces. A full CI expansion is then performed in the active space, including all configurations in the MCSCF calculation. The active space typically consists of a few of the highest energy occupied orbitals and lowest energy virtual orbitals from a HF reference. Further partitioning of the active space into domains with different excitation schemes is possible, known as the *restricted active space self-consistent-field* (RASSCF) method.

These CI methods all consider excitations from a single HF reference determinant. However, one can also consider excitations from the determinants contained in an MCSCF wavefunction. For example, CISD can be extended to include all singles and doubles excitations from *all* determinants contained in an MCSCF wavefunction. Such methods are termed *multireference configuration interaction* (MRCI). Of all the approaches considered so far, excluding the exact full CI, MRCI offers the highest quality wavefunction, but it comes at an extremely high computational cost.

One significant problem with any truncated CI method, including the analogous MCSCF and MRCI approaches, is their lack of *size consistency* and *extensivity*. Size consistency refers to a method's ability to correctly describe the energy of a collection of *non-interacting* particles. A size consistent method should predict that the energy of N non-interacting particles is exactly N times the energy of a single particle. Size extensivity, on the other hand, refers to systems of *interacting* particles and requires that the method correctly scales the energy in proportion to the number of particles.

Although the full CI is both size consistent and extensive, as an exact theory should be, this is not the case for any truncated CI or MCSCF method. Consequently, these methods are not suitable for describing macroscopic effects, both due to computational cost and size inconsistency, or for large molecular systems, as their accuracy deteriorates with an increasing number of particles (size extensivity). For a detailed explanation of this, see ref. 6.

Downloaded from http://books.rsc.org/books/edited-volume/chapter-pdf/1851664/bk9781837676200-00271.pdf by University of Kent user on 28 January 2025

1.4 Coupled-cluster methods

Truncated CI methods offer a conceptually straightforward approach to correcting the HF wavefunction and can be extended to multireference descriptions. However, their lack of size consistency and extensivity restricts their utility. This is because it is often desired to compare energies and properties between chemical systems that differ in number of atoms, for example, when following a reaction mechanism or the dissociation of a molecule. Since the full CI equation provides an exact description, it is desirable to devise approximations that, like the full CI method, do not suffer from these limitations.

This goal is indeed achieved through coupled-pair theories, with the gold standard being *coupled-cluster* (CC) (also known as *coupled-pair many-electron theory*). All CC methods are both size consistent and extensive. However, they are not variational, meaning that CC energies can sometimes be lower than the exact energy, and there is no definitive upper or lower bound against which to measure their accuracy.

At the core of such theories is the so-called *cluster expansion of the wavefunction*. Suppose we want to approximate the full CI expansion of the wavefunction by considering only doubly excited determinants while still maintaining size consistency. It can be shown that the formalism of a cluster expansion naturally arises from an attempt to do so, allowing higher excitation contributions to be included. Specifically, the coefficients for any 2*n*th-tuple excited determinants can be expressed in terms of *n* doubly excited coefficients. We can then consider adding triply excited determinants and describe higher excitation contributions in terms of them, and so on. However interesting this endeavour, it goes beyond the scope of this text and has already been demonstrated elsewhere.[6] To offer but a glimpse on the form of such an expansion, consider the following excitation operator $\mathcal{T}$:

$$\mathcal{T} = \mathcal{T}_1 + \mathcal{T}_2 + \mathcal{T}_3 + \cdots + \mathcal{T}_N \tag{14}$$

where N is the number of electrons in the system. The effect of the $\mathcal{T}_i$ operator on a given reference wavefunction is to generate all ith excited determinants. To write the full CI expansion, one needs only to apply $(1+\mathcal{T})$ to the HF reference and normalise accordingly. In the CC approach, however, one uses the exponential *ansatz,* instead:

$$\Phi_{\mathrm{CC}} = e^{\mathcal{T}}\Phi_{\mathrm{HF}} \tag{15}$$

Notice that both the CI and CC expansions are exact since they include all excited determinants, thereby covering the entire Hilbert space generated by the Hamiltonian. The difference lies in how these approaches group the contributions of each excitation. If one then expands $e^{\mathcal{T}}$ in a Taylor series, it yields:

$$\begin{aligned} e^{\mathcal{T}} &= 1 + \mathcal{T} + \frac{1}{2}\mathcal{T}^2 + \frac{1}{6}\mathcal{T}^3 + \cdots = \sum_{k=0}^{\infty}\frac{1}{k!}\mathcal{T}^k \\ &= 1 + \mathcal{T}_1 + \left(\mathcal{T}_2 + \frac{1}{2}{\mathcal{T}_1}^2\right) + \left(\mathcal{T}_3 + \mathcal{T}_2\mathcal{T}_1 + \frac{1}{6}{\mathcal{T}_1}^3\right) \\ &\quad + \left(\mathcal{T}_4 + \mathcal{T}_3\mathcal{T}_1 + \frac{1}{2}{\mathcal{T}_2}^2 + \frac{1}{2}\mathcal{T}_2{\mathcal{T}_1}^2 + \frac{1}{24}{\mathcal{T}_1}^4\right) + \cdots \end{aligned} \tag{16}$$

Downloaded from http://books.rsc.org/books/edited-volume/chapter-pdf/1851664/bk9781837676200-00271.pdf by University of Kent user on 28 January 2025

The last equality of the equation can be interpreted as follows: the first term returns the reference wavefunction, the second term includes all singly excited determinants, the third term (in parentheses) includes the doubly excited determinants, the fourth term includes the triply excited determinants, and so on. Note that at each excitation level, terms arising from combinations of lower-order excitations are present.

The major advantage of this approach becomes evident when we truncate the operator $\mathcal{T}$ at a certain excitation level. For instance, if we consider a CC with only singles and doubles excitations (CCSD), eqn (16) then becomes:

$$e^{\mathcal{T}_1+\mathcal{T}_2} = 1+\mathcal{T}_1+\left(\mathcal{T}_2+\frac{1}{2}\mathcal{T}_1{}^2\right)+\left(\mathcal{T}_2\mathcal{T}_1+\frac{1}{6}\mathcal{T}_1{}^3\right) + \left(\frac{1}{2}\mathcal{T}_2{}^2+\frac{1}{2}\mathcal{T}_2\mathcal{T}_1{}^2+\frac{1}{24}\mathcal{T}_1{}^4\right)+\cdots \tag{17}$$

By projecting the CCSD wavefunction against different singly excited determinants,[6,7] one can obtain the coefficients for the various contributions in the expansion of the wavefunction. Interestingly, contributions from higher than doubly excited determinants appear, even though the operator $\mathcal{T}$ is truncated at the doubles level. For example, the term $\mathcal{T}_2{}^2$ will generate quadruply excited determinants in the CCSD wavefunction. This feature ultimately makes CC methods more accurate, as well as size consistent and extensive. However, it also introduces non-linearity, leading to the non-variational nature of the method.

Additional pair theory methods, such as the *independent electron pair approximation* (IEPA) and the *coupled electron pair approximation* (CEPA)—a simplification of the CC approach—also exist but are not widely applicable. One reason is their relatively crude approximation and the fact that their energies are not invariant under unitary transformation of degenerate orbitals. More details on these methods can be found in ref. 6.

As it happens with the CI methods, one can extend the CC methods to multireference wavefunctions by using, for example, an MCSCF reference to construct an MRCC model. However, due to the complex nature of the CC expansion, this approach is less straightforward than MRCI. CC methods are considered the most accurate and advanced of the post-HF approaches, and many other levels of theory, including density functional theory (DFT) methods, are usually benchmarked against them.

1.5 Perturbative methods

CI and CC methods essentially rely on different *ansätze* to expand the wavefunction and then approximate the exact solution in a systematic way. The full expansions for both approaches are exact in the non-relativistic BO approximation framework. However, the approximations arising from the CC methods, unlike those from CI methods, are size consistent and extensive, though not variational. Another class of

Downloaded from http://books.rsc.org/books/edited-volume/chapter-pdf/1851664/bk9781837676200-00271.pdf by University of Kent user on 28 January 2025

methods for introducing correlation corrections to IPM wavefunctions, which share these same properties with CC methods, is based on many-body perturbation theory (MBPT). We will briefly cover the basic concept of this general theory, provide an understanding of the most popular version currently in use—namely, *Møller–Plesset perturbation theory* (MPPT)—, and discuss some of the multi-reference extensions to this approach. In doing so, we will refrain from entering the rather intricate mathematical aspects, and again, the interested reader can find these details in the cited sources.

The main concept in MBPT is the assumption that the Hamiltonian for the exact system under description can be partitioned into a main contribution ($\mathcal{H}_0$), for which we know the exact or approximate solution, and another contribution ($\mathcal{H}'$) which is small compared to $\mathcal{H}_0$. The latter is the perturbation introduced into the unperturbed (or reference) system. Suppose we know the solution for the unperturbed Hamiltonian $\mathcal{H}_0$:

$$\mathcal{H}_0|\chi_i\rangle = E_i|\chi_i\rangle, \quad i = 0,\ 1,\ 2, \ldots,\ \infty \tag{18}$$

Since $\mathcal{H}_0$ is Hermitian, the solution above forms a complete set of eigenfunctions $\{|\chi_i\rangle\}$. We now consider the total Hamiltonian:

$$\mathcal{H} = \mathcal{H}_0 + \lambda\mathcal{H}' \tag{19}$$

where we introduce an ordering parameter λ ($0 \leq \lambda \leq 1$) which will later be set to 1. With this strategy, we essentially build a Hamiltonian which can be continuously transformed from the unperturbed to the perturbed scenario by continuously increasing the value of λ. This continuity is reflected in the eigenvalues and eigenfunctions which solve the total system:

$$\mathcal{H}|\Phi_i\rangle = W_i|\Phi_i\rangle \tag{20}$$

We can, therefore, expand these solutions in powers of the parameter λ as:

$$W_i = \lambda^0 W_i^{(0)} + \lambda^1 W_i^{(1)} + \lambda^2 W_i^{(2)} + \lambda^3 W_i^{(3)} + \cdots \tag{21}$$

$$|\Phi_i\rangle = \lambda^0|\Phi_i^{(0)}\rangle + \lambda^1|\Phi_i^{(1)}\rangle + \lambda^2|\Phi_i^{(2)}\rangle + \lambda^3|\Phi_i^{(3)}\rangle + \cdots \tag{22}$$

Setting $\lambda = 0$ switches off the perturbation so that $\mathcal{H} = \mathcal{H}_0$. From eqn (20)–(22), we see that $|\Phi_i\rangle = |\Phi_i^{(0)}\rangle = |\chi_i\rangle$ and $W_i = W_i^{(0)} = E_i$. In other words, the solution is simply the unperturbed one (eqn (20)). The terms $|\Phi_i^{(1)}\rangle$, $|\Phi_i^{(2)}\rangle$, ... and $W_i^{(1)}$, $W_i^{(2)}$, ... are the first-, second-, and higher-order corrections to the wavefunctions and energies, respectively.

Let us use intermediate normalisation for the $\{|\Phi_i\rangle\}$, *i.e.* ensuring that $\langle\chi_i|\Phi_i\rangle = 1$ unless they are orthogonal. We can then introduce the expansion from eqn (22) in the TISE with the Hamiltonian defined in eqn (19) to obtain:

$$\begin{aligned}&(\mathcal{H}_0 + \lambda\mathcal{H}')(|\chi_i\rangle + \lambda^1|\Phi_i^{(1)}\rangle + \lambda^2|\Phi_i^{(2)}\rangle + \cdots)\\ &\quad = (E_i + \lambda^1 W_i^{(1)} + \lambda^2 W_i^{(2)} + \cdots)(|\chi_i\rangle + \lambda^1|\Phi_i^{(1)}\rangle + \lambda^2|\Phi_i^{(2)}\rangle + \cdots)\end{aligned} \tag{23}$$

Downloaded from http://books.rsc.org/books/edited-volume/chapter-pdf/1851664/bk9781837676200-00271.pdf by University of Kent user on 28 January 2025

Since this is valid for any value of λ, we can equate the coefficients of the same power n of λ to obtain:

$$\mathcal{H}_0|\chi_i\rangle = E_i|\chi_i\rangle \tag{24}$$

$$\mathcal{H}_0|\Phi_i^{(1)}\rangle + \mathcal{H}'|\chi_i\rangle = E_i|\Phi_i^{(1)}\rangle + W_i^{(1)}|\chi_i\rangle \tag{25}$$

$$\mathcal{H}_0|\Phi_i^{(2)}\rangle + \mathcal{H}'|\Phi_i^{(1)}\rangle = E_i|\Phi_i^{(2)}\rangle + W_i^{(1)}|\Phi_i^{(1)}\rangle + W_i^{(2)}|\chi_i\rangle \tag{26}$$

$$\vdots$$

and multiplying by $\langle\phi_i|$ with intermediate normalisation:

$$E_i = \langle\chi_i|\mathcal{H}_0|\chi_i\rangle \tag{27}$$

$$W_i^{(1)} = \langle\chi_i|\mathcal{H}'|\chi_i\rangle \tag{28}$$

$$W_i^{(2)} = \langle\chi_i|\mathcal{H}'|\Phi_i^{(1)}\rangle \tag{29}$$

$$\vdots$$

To obtain the various corrections to wavefunctions and energies, one must solve the above system of equations. Since they are integro-differential equations, we can use the fact the $\{|\chi_i\rangle\}$ forms a complete set and expand each $|\Phi_i^{(n)}\rangle$ in terms of this set. The solution for the first-order energy correction is already given by $\langle\chi_i|\mathcal{H}'|\chi_i\rangle$, which is the average value of the perturbation over the unperturbed wavefunctions. The second-order correction is:

$$W_i^{(2)} = \sum_{n\neq 0} \frac{\langle\chi_i|\mathcal{H}'|\chi_n\rangle\langle\chi_n|\mathcal{H}'|\chi_i\rangle}{E_i - E_n} \tag{30}$$

The details of the derivations, including higher-order corrections, can be found in ref. 6 and 7. While we do not show the explicit corrections to the wavefunction, the first-order correction can be calculated using the unperturbed wavefunctions and energies, which then yields the second-order correction for the energy. In summary, although the formulas for higher-order corrections become increasingly complex, they can all be expressed in terms of matrix elements of $\mathcal{H}'$ over the unperturbed $|\chi_i\rangle$ and corresponding energies E_i. This form of perturbation theory is called *Rayleigh–Schrödinger perturbation theory* (RSPT). It is a general and exact derivation, provided the initial assumptions are valid, and can be applied to any system as long as a suitable $\mathcal{H}'$ is devised. In fact, we will use this theory to treat the interaction of light with matter by approximating light as a time-dependent perturbation to a static quantum system (Section 2.3).

For now, our interest lies in using RSPT to introduce correlation to a reference wavefunction. The first task is to construct an appropriate total

Downloaded from http://books.rsc.org/books/edited-volume/chapter-pdf/1851664/bk9781837676200-00271.pdf by University of Kent user on 28 January 2025

Hamiltonian for the system, according to eqn (20), as a sum of a reference part for which we know at least an approximate solution and a small perturbation that correctly describes the effect we want to introduce as a correction. There are various ways to achieve this, but the most successful and widely available method is the Møller–Plesset (MP) approach. In this case, the unperturbed Hamiltonian is simply a sum of N Fock operators (eqn (9)) for each of the N electrons in the system:

$$\mathcal{H}_0 = \sum_i^N \mathcal{F}(i) = \sum_i^N h(i) + v^{\mathrm{HF}}(i) \tag{31}$$

As the summation runs through the N electrons, it counts the average electron interaction $v^{\mathrm{HF}}(i)$ twice. The perturbed Hamiltonian is then the exact electron–electron interaction operator minus this double-counted average contribution from the reference Fock Hamiltonian:

$$\mathcal{H}' = \sum_{i<j}^N \frac{1}{r_{ij}} - \sum_i^N v^{\mathrm{HF}}(i) \tag{32}$$

This choice of partition ensures that the solution is size consistent and extensive, which may not be the case for other partitioning schemes. However, such an $\mathcal{H}'$ cannot always be considered small in comparison to $\mathcal{H}_0$. If we look at eqn (20) and (27), we see that the zeroth-order energy is simply the sum of HF orbital energies $W^{(0)} = \sum_i^N E_i$, which accounts for the average electron–electron interaction twice. We recall that we introduced the subtraction of this factor in $\mathcal{H}'$, and that summation of $\frac{1}{r_{ij}}$ over different pairs of electrons in the HF determinant is again the same average interaction.

The first-order energy correction in MPPT only corrects the $\mathcal{H}_0$ energy, yielding the HF energy. Therefore, the first correction for correlation energy occurs on the second-order energy correction of the MPPT theory. If we designate the MPPT equations restricted to corrections up to order n by MPn, we have MP2 as the lowest level correction. The second order correction to the energy can be written in terms of the reference wavefunction and doubly excited determinants thereof.[6,7] The first-order correction to the wave-function also contains only contributions of the doubly excited determinants. Since knowledge of this correction allows for the calculation of the third-order energy correction, MP3 is readily available and is not much more expensive than MP2.

Higher-order corrections to energy require higher than first-order corrections to the wavefunction. Knowledge of the second-order correction to the wavefunction allows for MP4 and MP5 energy corrections, which include contributions of up to quadruply excited determinants. A similar pattern to CC and CI calculations arises here: more and more configurations are introduced to increase the accuracy of the model. While MP4 has a computational cost comparable to CISD, MP5 is already too costly for large systems.

Downloaded from http://books.rsc.org/books/edited-volume/chapter-pdf/1851664/bk9781837676200-00271.pdf by University of Kent user on 28 January 2025

Although MPPT methods offer an interesting alternative, their convergence is highly dependent on the reference wavefunction. If HF description of the system is not adequate, the convergence of MPPT energies can be erratic, with MP3 sometimes yielding poorer results than MP2, for example. A more detailed discussion about these convergence issues can be found in ref. 7–9.

For organometallic systems, the presence of heavy atoms often necessitates a multireference wavefunction as a starting point, posing particular challenges for MPPT methods due to their convergence issues. As with CI and CC methods, MPPT can be extended to the multireference scenario by employing an MCSCF wavefunction as the reference. The implementation of such methods is complicated by the choice of partition for the Hamiltonian. When an MCSCF wavefunction is used as the reference, one obtains multireference perturbation MRPT*n* methods, where *n* denotes the order of perturbation correction applied. If the reference is a CASSCF wavefunction, the methods are termed CASPT*n*. Only CASPT2 and CASPT3 have been widely implemented so far.

Another approach based on a CASSCF reference is the *N-electron valence state perturbation theory* (NEVPT*n*) class of methods.[10–12] These differ from CASPT*n* methods in the choice of reference Hamiltonian and perturbation. A detailed treatment of these methods is beyond the scope of this text, but a comparison and perspective on these approaches can be found in ref. 13.

Before we conclude our journey through the methods for correlation correction to the HF model, it is worth calling attention to explicitly correlated methods. A wavefunction built from a Slater determinant is based on one-particle orbitals. However, the correlation effects arise from the two particle terms in the electronic Hamiltonian. Thus, the methods discussed above suffer from a fundamental incompatibility with the electronic correlation phenomena: Slater determinants fail to model the exact wavefunction at short interelectronic distances. A solution is to explicitly consider terms dependent on the distances of electron pairs. Such approaches are motivated by Hylleraas' solution to the helium atom,[14] and are called R12 or F12 methods. They depend on the use of Gaussian basis functions for two electrons, known as Gaussian geminals, and include extremely costly many-electron integrals. This poses a big challenge for the simulation of big systems, but efforts are being made to improve their scalability. Given the complexity of these methods and the current scarce use for bigger molecular systems, we do not enter into the details, but refer the reader to two excellent reviews on these methods.[15,16] R12/F12 approaches are currently implemented for MP, CI and CC wavefunction *ansätze*.

1.6 Valence bond methods

All approaches to the electronic problem discussed so far have involved a molecular orbital (MO) picture of the wavefunction. In fact, the HF method—the fundamental MO model—has only been improved by applying more complicated wavefunction expansions through CI and CC

Downloaded from http://books.rsc.org/books/edited-volume/chapter-pdf/1851664/bk9781837676200-00271.pdf by University of Kent user on 28 January 2025

ansätze and/or by using perturbative methods to include electronic correlation. In the MO model, a molecule is viewed as composed by nuclei with a particular configuration (within the BO approximation) and molecular orbitals (and electronic density) delocalised throughout its entirety.

This picture is markedly different from the language chemists—particularly organic chemists—typically use to describe molecules and chemical reactions. Chemists often think about chemical bonds, their formation and cleavage, and the composition of molecules in terms of functional units or groups, relying fundamentally on a localised description of electrons. This perspective is preconised by the century-old concept of the chemical bond first introduced by Lewis, whereupon a pair of atoms is connected either covalently by an electron pair shared between only those atoms, or ionically by the electrostatic interaction arising from the localisation of the bonding electron pair in one of the two atomic centres.[17–19]

Valence bond (VB) methods, slightly older than MO methods, are much closer to this chemical description of molecular systems and are currently implemented in many quantum chemistry packages. The reason MO methods are more popular is that they are easier to implement and computationally cheaper to apply than VB methods. In the context of organometallic and transition metal systems, the application of VB methods is relatively rare. However, some recent studies have demonstrated their potential use in challenging systems such as metal–methyl ($M–CH_3$) complexes,[20] coinage metal halides,[21] gold complexes featuring interanion coinage bonds,[22] and metal–metal bonded systems.[23–25] Therefore, it is worth dedicating a few paragraphs to VB methods here, as they will become more and more approachable with increasing computational capacity and new means to improve the scalability of computations. Our goal is to provide a broad overview of the theoretical aspects in modern VB theory and the practical differences compared to MO methods.

When describing the HF model above, we argued that the IPM wavefunction *ansatz* in the form of a Slater determinant correctly accounts for the antisymmetric property of fermionic systems, but this alone does not ensure its correct form. Since the wavefunction is a solution to the electronic Hamiltonian, it must be a representation for the symmetric groups to which the Hamiltonian belongs. This includes both point group symmetry for the nuclear configuration and permutation group symmetry for the electrons as independent particles. The theory that explains the necessity of the latter is well-established, but its complexity meant that it was not a primary concern for many scientists developing these early electronic structure methods.[26–29]

The key point here is that a properly constructed VB wavefunction is superior to a Slater determinant (the core of the HF method), mainly because it is a representation of the S_N permutation group. The second characteristic that makes VB wavefunctions a better representation is the departure from the double occupancy of orbitals. Let us examine these properties in more detail.

Downloaded from http://books.rsc.org/books/edited-volume/chapter-pdf/1851664/bk9781837676200-00271.pdf by University of Kent user on 28 January 2025

The first application of a VB-type wavefunction was demonstrated by Heitler and London on the H_2 molecule.[30] In this model, a covalent bond between atoms A and B is formed from the respective (hybrid) atomic orbitals (HAOs) χ_A and χ_B by coupling them in a singlet and properly antisymmetrising by a spin term. The result is the Heitler–London (HL) wavefunction Φ_{cov} of the form:

$$\Phi_{cov} = (\chi_A\chi_B + \chi_B\chi_A)[\alpha\beta - \beta\alpha] = \Phi_{A-B} \tag{33}$$

where the order of the functions in each product indicates the electron coordinate. Note that in VB theory, the orbitals are, in principle, monoelectronic, meaning each electron is described by its own spatial function, and orbital double occupancy is not enforced. Similarly, ionic structures can be built for the same pair of atoms as follows:

$$\Phi_{ion(1)} = \chi_B\chi_B[\alpha\beta - \beta\alpha] = \Phi_{A^+B^-} \tag{34}$$

$$\Phi_{ion(2)} = \chi_A\chi_A[\alpha\beta - \beta\alpha] = \Phi_{A^-B^+} \tag{35}$$

In classical VB theory (CVBT), the molecule A–B is described by a linear combination of these three contributions:

$$\Phi_{AB} = C_1\Phi_{cov} + C_2\Phi_{ion(1)} + C_3\Phi_{ion(2)} \tag{36}$$

Such a wavefunction is a general CVBT representation as preconised by Pauling and Slater. For the H_2 molecule, C_1 is the largest coefficient, indicating that the covalent structure dominates. However, the presence of ionic contributions to the wavefunctions accounts for electronic effects (often termed "*static correlation*") that in the HF theory can only be included using CI approaches.[7] The same idea can be extended to larger molecules, though constructing the appropriate products, spin-functions, and antisymmetrisation becomes increasingly complex. Generally, one first constructs the spin function such that it is an eigenfunction of the total spin operator and is a representation of the S_N symmetric group. Then, one constructs the spatial wavefunction such that the total wavefunction is antisymmetric with respect to electron permutation. The details of this procedure and its underlying theory is presented in ref. 27 and 29.

In current applications of CVBT, the HAOs are expanded into an atomic orbital basis set, and the expansion coefficients, as well as the different configurations (as in eqn (36)) are optimised using an SCF procedure. This method is termed VBSCF. If the HAO coefficients for each independent structure in an equation like eqn (36) are allowed to be independently optimised, a *breathing orbital VB* (BOVB) method is being applied. While VBSCF improves the description compared to HF by including "static correlation" only, BOVB acts as a multireference method, thus also including "dynamic correlation", making it superior to VBSCF.

In the CVBT approach, the HAOs are essentially localised atomic orbitals. Another possibility is to use Coulson–Fischer HAOs. In this model, each HAO is allowed to possess a delocalisation "tail" by mixing a small

Downloaded from http://books.rsc.org/books/edited-volume/chapter-pdf/1851664/bk9781837676200-00271.pdf by University of Kent user on 28 January 2025

amount of the neighbouring atoms' HAOs. The wavefunction using these orbitals is then written as an HL covalent-like structure. This is the Coulson–Fischer (CF) *ansatz*. Notice that, by doing this, the orbitals are not orthogonal, which partially accounts for the high computational cost of such VB methods. For a molecule A–B, this would be eqn (33). The HAO coefficients are then optimised using an SCF procedure.

Once again, for larger molecules, constructing the CF wavefunction requires careful coupling of electrons in the bonds so that the total wavefunction is an eigenfunction of the total spin operator, a representation of the S_N group, and properly antisymmetric. Depending on the complexity of the molecule, there are many ways to achieve this. The number of spin-functions that can be generated for a coupling of N electrons with total spin S is given by:

$$f_S^N = \frac{(2S+1)N!}{\left(\frac{1}{2}N+S+1\right)!\left(\frac{1}{2}N-S\right)!} \tag{37}$$

For a methane molecule with 14 valence electrons, there are 14 spin-functions. A linear combination of all spin-coupling schemes, each multiplied by a proper spatial function and antisymmetrised, constitutes the spin-coupled VB (SCVB) theory developed by Gerratt *et al.*[31–33]

It is generally observed that one or a few of the spin-coupling terms dominate the SCVB description. Indeed, a few years earlier, Goddard *et al.* independently developed a similar approach, called *generalized valence bond* (GVB) theory.[34–38] Although completely equivalent to SCVB in its full form, which recently led VB practitioners to unify their names into a single framework known as *spin-coupled generalized valence bond* (SCGVB),[39] this wavefunction can be simplified in both its spatial and spin components.[39] An interesting application of SCGVB wavefunctions is in the development of the interference energy analysis (IEA) method,[40–43] which investigates the nature of the chemical bond as a manifestation of the quantum mechanical interference effect.

If the spin part is constructed so that covalent bonds are described by two electrons occupying two orbitals, one in each of the bonding atoms, coupled in a singlet pair, this spin function is called a perfect pairing spin function.[44] By enforcing strong orthogonality amongst orbitals from distinct electron pairs (but not those coupled in a bond or lone pair) and allowing core orbitals to be doubly occupied, we obtain what is called a *perfect pairing GVB* (GVB-PP) wavefunction. Although more computationally tractable than the full SCGVB wavefunction, such an approximation can lead to significant errors for some systems and must be used cautiously.

All VB methods can also be improved using CI, leading to methods such as VBCI, CASVB, and others available in various software packages. Although the implementation differs, the general idea is similar to that discussed for HF wavefunctions, allowing correlation corrections to be systematically added. A VB wavefunction as a starting point, however, is a much better reference than HF. In fact, the entire discussion about

Downloaded from http://books.rsc.org/books/edited-volume/chapter-pdf/1851664/bk9781837676200-00271.pdf by University of Kent user on 28 January 2025

"static" and "dynamic" correlation can be viewed as an unfortunate artifact of considering the HF wavefunction as a reference. It can be shown that SCGVB wavefunctions account for what is defined as static correlation by respecting the correct permutational symmetry and spin eigenfunction conditions. Thus, HF lacks this type of correlation because it is simply an incorrect *ansatz*. What remains, usually termed dynamic correlation, is the true correlation effect, not included in the SCGVB approach because it is, like HF, an IPM for the many-electron system. A better definition than eqn (11) for the correlation energy is then obtained by replacing the HF energy $E_{\mathrm{HF/CBS}}$ by the corresponding full SCGVB energy $E_{\mathrm{SCGVB/CBS}}$. More on this interesting discussion can be found in ref. 45–47 and more on VB methods can be found in ref. 25, 43, 48 and 49.

1.7 Density functional theory

Up to this point, we have discussed wavefunction methods exclusively. There is, however, a class of methods that is conceptually different but has proven to be exceptionally effective for many computational tasks at a fraction of the cost. Instead of solving the Schrödinger equation for the full wavefunction of a system and its corresponding energies, these methods exploit the fact that there is a univocal correspondence between the energy of a quantum system and its one-electron density. This framework is known as *density functional theory* (DFT), and its foundation is based on the Hohenberg–Kohn theorems. An introduction to DFT can be found in ref. 50. A more detailed treatment is provided in ref. 51 whilst a more rigorous mathematical treatment can be found in ref. 52.

Given the electronic wavefunction Φ of an N-electron system (solution of eqn (6), for example), the one-electron density $\rho(\boldsymbol{r})$ is defined as the integral of the square of the wavefunction over the N spin and $N-1$ spatial coordinates of the electrons, multiplied by the number of electrons in the system:

$$\rho(\boldsymbol{r}) = N \int\int \cdots \int |\Phi(\boldsymbol{x}_1,\ \boldsymbol{x}_2, \ldots, \boldsymbol{x}_N)|^2 \mathrm{d}\boldsymbol{s}_1 \mathrm{d}\boldsymbol{x}_2 \cdots \mathrm{d}\boldsymbol{x}_N \tag{38}$$

where $\boldsymbol{x}_i$ represents the joint spin $\boldsymbol{s}_i$ and spatial $\boldsymbol{r}_i$ coordinates of the electrons. Thus, $\rho(\boldsymbol{r})$ is a function of the spatial coordinates of a single electron and represents the spatial probability density of any one of the N electrons with an arbitrary spin, while the remaining electrons have arbitrary positions and spin. The integral of the density is $\int \rho(\boldsymbol{r})\mathrm{d}\boldsymbol{r} = N$.

The Hohenberg–Kohn theorems form the foundation of DFT. The first of the two theorems states that the ground-state of a system (and therefore its energy) is a univocal functional of the density $\rho(\boldsymbol{r})$. The second theorem establishes a variational principle for the ground-state energy. According to this principle, given any approximate electron density for a system, the calculated energy through the density functional will be higher than the exact energy, unless the density is exactly the ground-state density ρ_0. These theorems can also be extended to excited states.

Since the electronic density depends only on the three spatial coordinates of a single electron, regardless of the system's size, DFT offers a

Downloaded from http://books.rsc.org/books/edited-volume/chapter-pdf/1851664/bk9781837676200-00271.pdf by University of Kent user on 28 January 2025

promising, exact, and remarkably simple and inexpensive alternative compared to wavefunction methods, which depend on $3N$ coordinates. The main issue is that the exact functional connecting the electronic density to the energy is still unknown. Therefore, only approximate methods are available within this framework.

The only approximation scheme that provides useful results for molecular systems is the Kohn–Sham (KS) model for DFT. In this approach, the orbital picture is reintroduced, forcing us to go back to a $3N$ coordinate dependency of the energy. Thus, KS is similar to HF theory, although it is somewhat less costly and much more exact. The main idea in this model is the consideration that the HF method provides the exact kinetic energy for a system of non-interacting electrons. That said, the total kinetic energy can be partitioned in this exact part and a small correction for the interactions. By defining the one-electron KS operator as:

$$\mathcal{F}^{\mathrm{KS}} = -\frac{1}{2}\nabla^2 + V_{\mathrm{S}}(\boldsymbol{r}) \tag{39}$$

in analogy with the Fock operator, where V_{S} is an effective potential, one can use the same formalism as the HF (Section 1.2) to obtain a Slater determinant containing the spin–orbitals (χ_i) and energies for the non-interacting system of electrons. This set of spin–orbitals describes exactly a system of non-interacting electrons, with the exact kinetic energy given by $T_{\mathrm{S}} = -\frac{1}{2}\sum_i^N \langle\chi_i|\nabla^2|\chi_i\rangle$. The connection of this fictitious system with the real one is made by the choice of V_{S} such that the electronic density calculated from the KS spin–orbitals equals that of the real system. By computing most (*but not all*) of the real system's kinetic energy this way, the total KS functional $F[\rho(\boldsymbol{r})]$ can be partitioned into:

$$F[\rho(\boldsymbol{r})] = T_{\mathrm{S}}[\rho(\boldsymbol{r})] + J[\rho(\boldsymbol{r})] + E_{\mathrm{XC}}[\rho(\boldsymbol{r})] \tag{40}$$

where $J[\rho(\boldsymbol{r})] = \frac{1}{2}\int\int \frac{\rho(\boldsymbol{r}_1)\rho(\boldsymbol{r}_2)}{r_{12}}\mathrm{d}\boldsymbol{r}_1\mathrm{d}\boldsymbol{r}_2$ is the classical Coulomb interaction, and $E_{\mathrm{XC}}[\rho(\boldsymbol{r})]$, the exchange–correlation (XC) functional, contains all the non-classical electrostatic interactions plus the unknown part of the electronic kinetic energy. If we were to discover the exact form of this functional, the energy obtained in the KS approach would be the exact energy. Bear in mind, though, that we *would not* obtain the *wavefunction* for the system.

The XC part of the KS functional holds all the approximations of the method, including electronic correlation. This is where most of the current efforts in the development of DFT methods are focused. The task of the user is to judiciously choose the appropriate DFT functional for the task at hand. The number of available functionals is bewildering, and discussing their intricacies in detail is beyond the scope of this chapter. Instead, we aim to provide a rough classification of these functionals and some conceptual foundations. We will also discuss some applications in the context of organometallic systems in Section 3.

Downloaded from http://books.rsc.org/books/edited-volume/chapter-pdf/1851664/bk9781837676200-00271.pdf by University of Kent user on 28 January 2025

The simplest strategy to devise an XC functional is the *local density approximation* (LDA). This model is based on a uniform electron gas—a model where electrons move in the field of a continuous positive charge distribution, in a way that the total system is neutral. The number N of electrons and the volume V of the system are infinite, while the electronic density N/V remains finite and constant throughout. The XC functional for such a system can be written as a simple integral of the electronic density $\rho(\boldsymbol{r})$ multiplied by the exchange–correlation energy of the electron gas:

$$E_{\mathrm{XC}}^{\mathrm{LDA}}[\rho] = \int \rho(\boldsymbol{r})\epsilon(\rho(\boldsymbol{r}))\mathrm{d}\boldsymbol{r} \tag{41}$$

The results obtained with such functionals are comparable to or even better than those obtained by the HF method. An improvement of this method is the *generalised gradient approximation* (GGA). In this approach, the information coming from the electron gas density is supplemented by the gradient of the density, $\nabla\rho(\boldsymbol{r})$. It considers the fact that the electronic density of a real electronic system, contrary to that of an electron gas, is not homogenous. This is achieved by recognising that LDA can be regarded as the first-order term of a Taylor expansion of E_{XC} in terms of the density. This is the so-called *gradient expansion approximation* (GEA), and GGA functionals are obtained from this by certain manipulations to ensure that *exchange–correlation hole* properties are respected.[51] Such functionals are not derived entirely from first principles but include a series of parameters fitted to experimental data, as is the case with the remaining functionals below. For this reason, certain authors refrain from labelling many DFT methods as *ab initio*.

Building on the Taylor expansion mentioned earlier, one can further improve the GGA approach by including the Laplacian of the density, $\nabla^2\rho(\boldsymbol{r})$. Functionals that incorporate this additional term, although not directly constructed by the simple addition of the Laplacian of the density, are known as meta-GGA functionals. These functionals typically perform better than LDA and GGA functionals for molecular systems, and more details on their implementation can be found in ref. 52.

Another class of functional that generally outperforms GGAs, and often surpasses meta-GGAs, are the *hybrid* or *hyper-GGA* functionals. These functionals leverage the fact that the exchange part of the XC energy can be computed exactly for a Slater determinant using the HF approach. One can thus use this parcel of the energy and only approximate the correlation part in the functional. Although this partition is a fictitious mathematical construct—the XC term is inherently a single entity—a careful partitioning scheme can yield effective XC functionals by mixing the HF exchange energy with LDA, GGA, or even meta-GGA XC energies. In fact, one of the most popular DFT functionals, B3LYP, is an example of this approach.

Two of the major inaccuracies of DFT calculations are the self-interaction error and the absence of long-range correlation effects, responsible for London's dispersion forces.[53,54] Although the omission of long-range correlation is an inherent limitation of DFT, it can now be easily addressed by applying several established dispersion correction

Downloaded from http://books.rsc.org/books/edited-volume/chapter-pdf/1851664/bk9781837676200-00271.pdf by University of Kent user on 28 January 2025

methods. Prominent among these is Grimme's D3 method[55]—which can be applied using either the initial damping function, D3(0),[56] or the updated Becke–Johnson (BJ) damping function—or its more recent version D4.[57]

An even higher level of improvement is achieved with *double hybrid* functionals. These functionals not only use information from occupied orbitals in the form of the HF exchange energy but also incorporate information from all the KS orbitals. Specifically, they include an MP2 component of the energy, obtained by applying the formalism described in Section 1.5 to the KS Slater determinant. These methods have a higher computational cost than the previous ones because of the extra computations required for the MP2 energy and the convergence difficulties associated with such a perturbative approach, as discussed in Section 1.5.

When treating excited-states *via* time-dependent DFT (TDDFT) methods (see Section 2.4), it has been observed that many functionals fail to accurately describe charge transfer and Rydberg states. This issue arises partly because DFT tends to artificially favour delocalised systems over localised ones. Additionally, the long-range behaviour of the electronic energy is generally misrepresented due to an imbalance between the density-based Coulomb ($J[\rho(\boldsymbol{r})]$) and exchange (HF part in hybrid functionals) components and the approximate XC potential. A solution to this problem is brought by the class of *range-separated* functionals. In this strategy, the electron–electron Coulomb operator for the exchange energy (*only*) is split into short-range and long-range components, using different approaches for each. Typically, a density exchange functional is used for the short-range part, while the exact HF part is used for the long-range part. The two domains are interpolated using an ω parameter, which can be tuned for specific systems by applying Koopman's theorem.[58]

Fig. 1 presents a schematic hierarchy of DFT functional classes, commonly referred to as Jacob's ladder.[59]

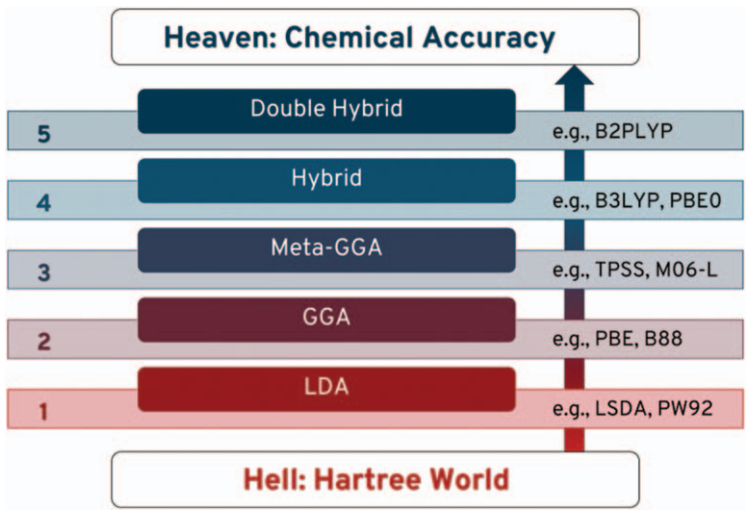


Fig. 1 The DFT Jacob's ladder.

Downloaded from http://books.rsc.org/books/edited-volume/chapter-pdf/1851664/bk9781837676200-00271.pdf by University of Kent user on 28 January 2025

1.8 Relativistic corrections

All of the theoretical treatment above assumed a non-relativistic scenario. This is, of course, an approximation. The fundamental problem with the non-relativistic treatment of a quantum system is that the Schrödinger equation is not invariant under a Lorentz transformation of space-time coordinates—a fundamental requirement of special relativity. The Dirac equation can be seen as a generalisation of the Schrödinger equation that does respect this property. It also accounts for the fact that the mass of a particle increases with increasing velocity. This implies that an electron orbiting a heavier nucleus will have a higher velocity, and therefore a higher mass, compared to one orbiting a lighter nucleus. The outcome is either a contraction or an expansion of the orbitals.

Another consequence of the Dirac equation is that the total angular momentum of an electronic system is no longer defined solely by the orbital angular momentum (L), but by a combination of this with the spin angular momentum (S), giving rise to a J term. In other words, the L and S operators do not commute with the Hamiltonian anymore, but J does. This is the spin–orbit coupling phenomenon. As a result, orbitals (and the entire system) do not have well-defined spin states, and the pure s, p, *etc.* non-relativistic orbitals now mix. In the presence of an external electromagnetic field, other relativistic effects also arise.

Additionally, the use of a Coulomb potential to describe the electric interactions is no longer valid in the relativistic realm since such interactions are instantaneous and thus violate the universal speed limit of light. The correct treatment of electric interactions would have to start from a quantum electrodynamics perspective, but modifications of the Coulomb potential can be made through approximation schemes, such as the inclusion of a Breit operator.

Here, we point out that relativistic corrections become increasingly important for systems containing heavier atoms. Since many organometallic systems contain metals beyond the fourth row of the periodic table, it is crucial to consider these effects. The simplest way to account for relativistic effects is by including relativistic *effective core potentials* (ECPs) to the basis set. Examples of such basis sets include the Los Alamos National Laboratory 2 double zeta (LANL2DZ)[60] and the Weigend and Ahlrichs def2 family of basis sets.[61]

Another relatively straightforward approach is to approximate a relativistic Hamiltonian using methods such as the *zeroth-order regular approximation* (ZORA) or the *first-order regular approximation* (FORA).[62–64] Both methods include spin–orbit coupling and scalar relativistic effects, which account for the mass dependency on velocity and the relativistic movement of electrons, known as the Darwin correction.

Perturbative operators have also been devised to include corrections to the non-relativistic solution.[7] Since this strategy results in complicated equations, it is sometimes easier to directly solve the Dirac equation. Using spinors (relativistic spin–orbitals) in a Slater determinant, one can write a relativistic *ansatz* like the HF wavefunction for the Dirac equation, and this is known as the *Dirac–Fock* (DF) method.

Downloaded from http://books.rsc.org/books/edited-volume/chapter-pdf/1851664/bk9781837676200-00271.pdf by University of Kent user on 28 January 2025

The so-called *two-component* methods are also available. The reason for this name is that a relativistic wavefunction has four components, which can be separated into one pair called the large component, and another pair called the small component, which depend on one another. Two-component methods use unitary transformations to separate these components, making them (quasi-)independent and allowing them to be solved separately. Examples of this approach include the *exact two-component* (X2C)[7] and *Douglas–Kroll–Hess* (DKH) methods.[65,66] A notable application of these methods for describing the spectroscopic properties of organometallic systems can be found in the ReSpect (Relativistic Spectroscopy) program, accessible at https://www.respectprogram.org/.

2 Excited state methods

Having discussed the various levels of theory for solving the static electronic problem, we are now positioned to address the problem of excited states and their properties. These methods are sometimes referred to as dynamic methods because many are derived from the TDSE (eqn (1)). However, this nomenclature should not be confused with dynamics simulations such as molecular dynamics or quantum (adiabatic or non-adiabatic) dynamics.

Our focus here will be on methods that allow us to calculate energies and molecular properties resulting from the interaction of UV and visible light with matter, thus altering their vibronic (electronic coupled with vibrational) states. The class of time-dependent methods (and much of the theory discussed here) however, is much broader. With proper formulation, they can account for many types of time-dependent phenomena arising from magnetic and electric fields interacting with matter.

The case of electronic time-dependent methods is complicated by the fact that a general theory should consider the relativistic and quantum nature of both the photons and the molecular systems. Such a treatment falls within the realm of quantum electrodynamics or, more generally, QFT. Since routine methods at this level are not easily available, we will use an approximate, semi-classical theory. For exact electronic methods, we started from a non-relativistic perspective, although it is possible to correct for, or approximate many, relativistic effects, as discussed in Section 1.8. We will continue with this assumption for the electronic wavefunction.

Additionally, we will treat light classically, as oscillations of an electromagnetic field. Since the magnetic component is much smaller than the electric component, we will disregard its effect and use the dipole approximation (see below). As usual, we will be working within the BO approximation, although these methods can be expanded to account for non-Born–Oppenheimer effects.

2.1 ΔSCF methods

Conceptually, the simplest way to consider excited states is by directly constructing their wavefunctions and proceeding analogously to the ground state calculations discussed above. If the excited state under consideration has a different (spatial and spin) symmetry than the ground state, this approach is straightforward. However, if it has the same

Downloaded from http://books.rsc.org/books/edited-volume/chapter-pdf/1851664/bk9781837676200-00271.pdf by University of Kent user on 28 January 2025

symmetry of the ground state, the SCF or variational procedure will almost invariably return the ground state, as it is the lowest energy state of that symmetry. There are special techniques to obtain these excited states directly, but they are difficult and possess several technical problems.[67]

It is often the case that excited states cannot be properly described by a single reference wavefunction, thus necessitating the use of MCSCF wavefunctions. Correlation can then be included by the various methods described above. Excitation energies can be calculated by taking the difference between the excited and ground state energies directly (ΔSCF approach). Molecular properties can also be calculated from various energy derivative techniques directly applied to the appropriate wavefunctions.

HF, MP*n* and CC type wavefunctions are not well-suited for calculating excited state *wavefunctions* in such a way because of their unsuitable references. We have already seen that CI methods straightforwardly give excited state wavefunctions as eigenstates of the CI matrix with higher energy eigenvalues. In fact, in most software packages, when HF is selected for excited states, what actually happens is that the CIS matrix is diagonalised to yield the excited states. However, care must be taken when choosing the CI level, as many excited states need two or more excited determinants for proper description. Even low-lying excited states of simple organic molecules may need at least CISDTQ wavefunctions for accurate description;[7,68] this is even more crucial for organometallic compounds.

Additionally, dynamic correlation can only be included in singly excited states by considering at least doubly excited determinants or by including perturbative corrections to the excited state wavefunctions. Thus, CIS excited states are described with a quality similar to HF ground states. This demanding level is often prohibitive except for small organic molecules. The methodology described in the next sections will offer more robust and cost-effective options for calculating excited state properties and wavefunctions. Nevertheless, CASPT2 or NEVPT2 models are deemed as gold standards for benchmarking excited state calculations whenever possible. It is worth noting that, in general, the higher the excited states considered, the higher the error.

2.2 TDSE representations

A series of formalisms have been developed for obtaining dynamic properties of molecular systems from the TDSE. The following methods will be considered: (1) *time-dependent perturbation theory* (TDPT), which will then lead to the most popular excited state method, namely, *linear response theory* (LRT), sometimes also called *random phase approximation* (RPA); (2) *variational methods*, to obtain time-dependent wavefunctions and properties, which form the basis for time-dependent HF (TDHF) and time-dependent DFT (TDDFT) methods; (3) *propagator methods*, which circumvent the need to calculate time-dependent wavefunctions; (4) *equation-of-motion* (EOM) methods; and (5) the *algebraic diagrammatic construction* (ADC) family of methods.

For each formalism, it becomes evident that certain representations of the TDSE are more suitable than others, and therefore, we will define

Downloaded from http://books.rsc.org/books/edited-volume/chapter-pdf/1851664/bk9781837676200-00271.pdf by University of Kent user on 28 January 2025

them here. As usual, we will not dive into the mathematical intricacies of the methods but focus on the essentials to give a superficial understanding of the concepts and critically assess each option.

We have seen (Section 1.1) that the TDSE equation can be solved by separating the total wavefunction into the product of a time-independent wavefunction $\psi(\boldsymbol{x})$ and a time-dependent factor $f(t) = \mathrm{e}^{-\frac{i}{\hbar}E_t t}$ (eqn (2)), where we denoted the combined spatial (and spin) coordinates by $\boldsymbol{x}$. More generally, we can define the operator $\mathrm{e}^{-\frac{i}{\hbar}\mathcal{H}t}$, where $\mathcal{H}$ is the time-independent Hamiltonian for the system, which maps $\Psi(\boldsymbol{x}, t=0)$ into $\Psi(\boldsymbol{x}, t)$. This is seen by the exact separation of variables procedure and integration of the TDSE:

$$\int_{\Psi(\boldsymbol{x},t=0)}^{\Psi(\boldsymbol{x},t)} \frac{\mathrm{d}\Psi}{\Psi} = \int_0^t \frac{1}{i\hbar}\mathcal{H}\mathrm{d}t' \tag{42}$$

$$\ln\frac{\Psi(\boldsymbol{x},\ t)}{\Psi(\boldsymbol{x},0)} = -\frac{i}{\hbar}\mathcal{H}t \tag{43}$$

from which:

$$\Psi(\boldsymbol{x},\ t) = \mathrm{e}^{-\frac{i}{\hbar}\mathcal{H}t}\Psi(\boldsymbol{x},0) \tag{44}$$

The operator thus defined is called the *evolution operator* or *propagator* and is sometimes denoted as $U(t)$. Differentiating $U(t) = \mathrm{e}^{-\frac{i}{\hbar}\mathcal{H}t}$, we see that $U(t)$ satisfies the TDSE:

$$i\hbar\frac{\mathrm{d}U(t)}{\mathrm{d}t} = \mathcal{H}U(t) \tag{45}$$

Eqn (44) is strictly valid for a time-independent Hamiltonian, but eqn (45) is valid even for a time-dependent one. In the scenario described above, consider the expectation value of an operator $\mathcal{A}$ as a function of time:

$$\langle\mathcal{A}\rangle_t = \langle\Psi(\boldsymbol{x},t)|\mathcal{A}|\Psi(\boldsymbol{x},t)\rangle = \left\langle \mathrm{e}^{-\frac{i}{\hbar}\mathcal{H}t}\Psi(\boldsymbol{x},0)\middle|\mathcal{A}\middle|\mathrm{e}^{-\frac{i}{\hbar}\mathcal{H}t}\Psi(\boldsymbol{x},0)\right\rangle \tag{46}$$

This result is expressed in the Schrödinger picture, where the time dependence of the expectation value is included solely on the state vectors $|\Psi\rangle$, while the operators are stationary. One can define a different representation where the state vectors are kept constant in time, but the operators evolve with time. Such a representation is called the Heisenberg picture. It is accomplished by defining the Heisenberg picture state vector $|\Psi_{\mathrm{H}}\rangle$ in terms of the Schrödinger picture state vector $|\Psi_{\mathrm{S}}\rangle$ as:

$$|\Psi_{\mathrm{H}}(\boldsymbol{x},t)\rangle = |\mathrm{e}^{\frac{i}{\hbar}\mathcal{H}t}\Psi_{\mathrm{S}}(\boldsymbol{x},t)\rangle \tag{47}$$

From eqn (44), we see that $|\Psi_{\mathrm{H}}(\boldsymbol{x},\ t)\rangle = |\Psi_{\mathrm{S}}(\boldsymbol{x},0)\rangle = |\Psi_{\mathrm{H}}(\boldsymbol{x},0)\rangle$, thus proving that $|\Psi_{\mathrm{H}}(\boldsymbol{x},t)\rangle$ is stationary in time. The connection between an operator $\mathcal{A}_{\mathrm{S}}$ in the Schrödinger picture and its counterpart in the Heisenberg picture is given by:

$$\mathcal{A}_{\mathrm{H}}(t) = \mathrm{e}^{\frac{i}{\hbar}\mathcal{H}t}\mathcal{A}_{\mathrm{S}}\mathrm{e}^{-\frac{i}{\hbar}\mathcal{H}t} \tag{48}$$

Downloaded from http://books.rsc.org/books/edited-volume/chapter-pdf/1851664/bk9781837676200-00271.pdf by University of Kent user on 28 January 2025

The expectation value of $\mathcal{A}$ in any of the pictures is, of course, the same since they only differ in representation.

A somewhat intermediate representation between the Schrödinger and Heisenberg representations is the interaction picture. Consider a partitioning of the full Hamiltonian as $\mathcal{H} = \mathcal{H}_0 + V$, as we have seen when discussing perturbative methods, where $\mathcal{H}_0$ is a Hamiltonian for which the time evolutions are known. The interaction picture wavefunction is defined by:

$$|\Psi_{\mathrm{I}}(\boldsymbol{x}, t)\rangle = \left|\mathrm{e}^{\frac{i}{\hbar}\mathcal{H}_0 t}\Psi_{\mathrm{S}}(\boldsymbol{x}, t)\right\rangle = \left|\mathrm{e}^{\frac{i}{\hbar}\mathcal{H}_0 t}\mathrm{e}^{-\frac{i}{\hbar}\mathcal{H}t}\Psi_{\mathrm{S}}(\boldsymbol{x}, 0)\right\rangle \tag{49}$$

If most of the time evolution is due to $\mathcal{H}_0$ (*i.e.* V is considered a perturbation) then the forward propagation under $\mathcal{H}$ will be counteracted by the backward propagation due to $\mathcal{H}_0$. Thus, Ψ_{I} undergoes much less time evolution than Ψ_{S} in the same situation.

2.3 Time-dependent perturbation theory

Arguably, the most popular theory for treating time-dependent quantum phenomena is perturbation theory. We have encountered its principles when discussing MBPT above (Section 1.5). One can outline a time-dependent formalism in a remarkably similar way to the static case. We start by partitioning the total time-dependent Hamiltonian in two parts according to $\mathcal{H} = \mathcal{H}_0 + \lambda\mathcal{H}_1$. Here, $\mathcal{H}_0$ is a time-independent Hamiltonian for which we know at least an approximate solution for its time evolution. $\mathcal{H}_1$ is regarded as a perturbation, *i.e.* the effect of $\mathcal{H}_1$ in the evolution of the system is much smaller than the effect of $\mathcal{H}_0$. The parameter λ is introduced as an ordering parameter, similar to its role in MBPT, and will ultimately be set to unity.

We proceed by expanding the wavefunction $\Psi(\boldsymbol{x},t)$ in a power series in λ, substituting the expansion into the TDSE, and equating like powers of λ. This process yields a series of equations for the different orders of perturbation corrections to the wavefunction. Solving the equations and performing some algebraic manipulations, one arrives at various expressions for the corrections to the wavefunction.[5]

$$\Psi^{(1)}(\boldsymbol{x}, t) = \frac{1}{i\hbar}\int_{t_0}^{t} \mathrm{d}t' \mathrm{e}^{-\frac{i}{\hbar}\mathcal{H}_0(t-t')}\mathcal{H}_1(t')\mathrm{e}^{-\frac{i}{\hbar}\mathcal{H}_0(t'-t_0)}\Psi^{(0)}(\boldsymbol{x}, t_0) \tag{50}$$

$$\begin{aligned}\Psi^{(2)}(\boldsymbol{x}, t) = \frac{1}{(i\hbar)^2}\int_{t_0}^{t} \mathrm{d}t' \int_{t_0}^{t'} \mathrm{d}t'' \mathrm{e}^{-\frac{i}{\hbar}\mathcal{H}_0(t-t')}\mathcal{H}_1(t')\mathrm{e}^{-\frac{i}{\hbar}\mathcal{H}_0(t'-t'')}\mathcal{H}_1(t'') \\ \times \mathrm{e}^{-\frac{i}{\hbar}\mathcal{H}_0(t''-t_0)}\Psi^{(0)}(\boldsymbol{x}, t_0)\end{aligned} \tag{51}$$

Further corrections can be derived, although the expressions become increasingly complex to integrate. Here, we have assumed that $\Psi(\boldsymbol{x},t_0) = \Psi^{(0)}(\boldsymbol{x},t_0)$, *i.e.* the total wavefunction at the initial time is the unperturbed wavefunction under the effect of $\mathcal{H}_0$ only. If the perturbation

Downloaded from http://books.rsc.org/books/edited-volume/chapter-pdf/1851664/bk9781837676200-00271.pdf by University of Kent user on 28 January 2025

is finite in time, such as the case of a laser pulse (*e.g.* pump–probe experiments), we can set $t_0 = 0$, where the origin of time is set before the perturbation takes effect. If one is treating a prolonged exposure to an electric field (*e.g.* regular UV-Vis spectroscopy), it is better to consider the perturbation as always-existing or steady-state. In this case, we set $t_0 \rightarrow -\infty$.

A different approach to perturbation theory can be taken. Above, we found a perturbative correction to the *wavefunction* in the *Schrödinger picture*, following a similar approach as the RSPT. Alternatively, one can also use the *interaction picture* to search for corrections to the Schrödinger picture *propagator* $U(t,t_0)$, since in this representation the perturbation is entirely due to the perturbation operator. For this, we define the zeroth-order propagator $U^{(0)}(t,t_0)$, associated with $\mathcal{H}_0$, which satisfies the TDSE:

$$i\hbar \frac{\partial}{\partial t} U^{(0)}(t, t_0) = \mathcal{H}_0 U^{(0)}(t, t_0) \tag{52}$$

We can then define an interaction picture propagator (see the definition of the interaction picture wavefunction, eqn (49))

$$U_{\mathrm{I}}(t, t_0) = \mathrm{e}^{\frac{i}{\hbar}\mathcal{H}_0(t-t')} \mathrm{e}^{\frac{i}{\hbar}\mathcal{H}(t-t')} = U^{(0)\dagger}(t, t_0) U(t, t_0) \tag{53}$$

which satisfies the following TDSE:

$$i\hbar \frac{\partial}{\partial t} U_{\mathrm{I}}(t, t_0) = \mathcal{H}_1 U_{\mathrm{I}}(t, t_0) \tag{54}$$

where:

$$H_{\mathrm{I}}(t) = \mathrm{e}^{\frac{i}{\hbar}\mathcal{H}_0(t)} H_1(t) \mathrm{e}^{-\frac{i}{\hbar}\mathcal{H}_0(t)} \tag{55}$$

is the interaction picture Hamiltonian. Eqn (54) can be iteratively solved exactly to arrive at:

$$U_{\mathrm{I}}(t, t_0) = 1 + \sum_{n=1}^{\infty} U_{\mathrm{I}}^{(n)}(t, t_0) \tag{56}$$

where:

$$\begin{aligned} &U_{\mathrm{I}}^{(n)}(t, t_0) \\ &= \frac{1}{(i\hbar)^n} \int_{t_0}^{t} \mathrm{d}\tau_n \int_{t_0}^{\tau_n} \mathrm{d}\tau_{n-1} \cdots \int_{t_0}^{\tau_2} \mathrm{d}\tau_1 \mathcal{H}_1(\tau_n) \mathcal{H}_1(\tau_{n-1}) \cdots \mathcal{H}_1(\tau_1) U_{\mathrm{I}}(t, t_0) \end{aligned} \tag{57}$$

The causality constraint $t > \tau_n > \tau_{n-1} > \cdots > \tau_1 > t_0$ is applied. By setting $U_{\mathrm{I}}(\tau_1, t_0) = 1$, which amounts to $\mathcal{H} = \mathcal{H}_0$, and replacing in eqn (56) and (55), one can use eqn (53) to derive the perturbation expansion for the Schrödinger picture propagator:

$$U(t, t_0) = U^{(0)}(t, t_0) + \sum_{n=1}^{\infty} U^{(n)}(t, t_0) \tag{58}$$

Downloaded from http://books.rsc.org/books/edited-volume/chapter-pdf/1851664/bk9781837676200-00271.pdf by University of Kent user on 28 January 2025

where:

$$U^{(n)}(t,t_0)=\frac{1}{(i\hbar)^n}\int_{t_0}^{t}\mathrm{d}\tau_n\int_{t_0}^{\tau_n}\mathrm{d}\tau_{n-1}\cdots\int_{t_0}^{\tau_2}\mathrm{d}\tau_1 U^{(0)}(t,\tau_n)$$
$$\times\mathcal{H}_1(\tau_n)U^{(0)}(\tau_n,\tau_{n-1})\mathcal{H}_1(\tau_{n-1})\cdots U^{(0)}(\tau_2,\tau_1)\times\mathcal{H}_1(\tau_1)U^{(0)}(\tau_1,t_0) \quad (59)$$

If we substitute $U^{(0)}(t,t')=\mathrm{e}^{-\frac{i}{\hbar}\mathcal{H}_0(t-t')}$ into eqn (58) and (59) and apply the results to $\Psi^{(0)}(t_0)$, we arrive at the same expressions in eqn (50) and (51) for the time-dependent corrections to the wavefunction. Notice that each of the approaches just described arrive at the same result, which is a correction to the total wavefunction in terms of an unperturbed wavefunction $\Psi^{(0)}$. In practice, we do not have an exact solution of the TDSE for $\Psi^{(0)}$. Therefore, our corrections will be applied on an imperfect reference. Since the time-dependent $\Psi^{(0)}$ will always be represented by a time-independent imperfect reference (such as a HF or CI wavefunction), perturbative methods will exacerbate the flaws of this reference, demanding care in its application.

By adequately considering different forms of perturbation and using the basic perturbation formulas outlined above, various spectroscopic techniques can be simulated, and the wavefunction dynamics and other properties can be obtained. To illustrate, let us consider one-photon absorption and emission spectroscopies. We will provide a sketch of the theory, and more details can be found elsewhere.[5,68] We assume the BO approximation and describe our system as composed of two states: the initial state with Hamiltonian $\mathcal{H}_\mathrm{a}$, which is typically the ground state but not necessarily, and the final excited state after absorption of a photon with Hamiltonian $\mathcal{H}_\mathrm{b}$. In the dipolar approximation, the interaction of matter with light is considered to be independent of position, and the potential due to the light is $-\boldsymbol{\mu}\cdot\boldsymbol{\epsilon}(t)$, where $\boldsymbol{\mu}$ is the molecular dipole moment and $\boldsymbol{\epsilon}(t)$ is the electric component of the radiation.

Here, we will consider a continuous wave, such that $\epsilon(t)=\epsilon_0\cos(\omega t)=\frac{1}{2}\epsilon_0(\mathrm{e}^{i\omega t}+\mathrm{e}^{-i\omega t})$. We momentarily disregard the vectorial nature of $\boldsymbol{\mu}$ and $\boldsymbol{\epsilon}$. We can then define, in the perturbation regime, $\mathcal{H}=\mathcal{H}_0+\mathcal{H}_1$, such that:

$$H_0=\begin{pmatrix}H_\mathrm{a} & 0\\ 0 & H_\mathrm{b}\end{pmatrix} \quad (60)$$

$$H_1=\begin{pmatrix}0 & -\frac{1}{2}\mu\epsilon_\mathrm{I}\mathrm{e}^{-i\omega t}\\ -\frac{1}{2}\mu\epsilon_\mathrm{S}\mathrm{e}^{i\omega t} & 0\end{pmatrix} \quad (61)$$

Here, $-\frac{1}{2}\mu\epsilon_\mathrm{S}\mathrm{e}^{i\omega t}$ is related to the emission (scattering) process, while $-\frac{1}{2}\mu\epsilon_\mathrm{I}\mathrm{e}^{-i\omega t}$ is related to the absorption of the incident light. If we assume

Downloaded from http://books.rsc.org/books/edited-volume/chapter-pdf/1851664/bk9781837676200-00271.pdf by University of Kent user on 28 January 2025

that before excitation there is no amplitude in the excited state, we can write the zeroth-order wavefunction as:

$$\Psi^{(0)}(\boldsymbol{x},0)=\begin{pmatrix}\Psi_{\mathrm{a}}\\0\end{pmatrix} \tag{62}$$

Substituting the equations above into our result for the first-order correction to the wavefunction (eqn (50)) and solving, one arrives at the following result (omitting a phase factor; see ref. 5 for details):

$$\Psi^{(1)}(\boldsymbol{x},t)=\frac{1}{2i\hbar}\int_{-\infty}^{t}\mathrm{e}^{-\frac{i}{\hbar}\mathcal{H}_{\mathrm{b}}(t-t')}\left\{\mu\cdot\epsilon_{\mathrm{I}}\mathrm{e}^{-i\omega_{\mathrm{I}}t'}\right\}\mathrm{e}^{-\frac{i}{\hbar}E_i t'}\Psi_i(\boldsymbol{x},-\infty)\mathrm{d}t' \tag{63}$$

with $\Psi_i(\boldsymbol{x},-\infty)$ being an eigenfunction of the ground state Hamiltonian $\mathcal{H}_{\mathrm{a}}$. Now, the absorption spectrum can be defined as the ratio of the number of photons absorbed per unit time to the number of incident photons per unit area per unit time. The number of photons absorbed per unit time is equal to the rate of change of the excited state population, which, in the perturbative limit, is given by the time derivative of $\langle\Psi^{(1)}(\boldsymbol{x},t)|\Psi^{(1)}(\boldsymbol{x},t)\rangle$. Using eqn (63) and differentiating this definition with respect to t, we arrive at the expression for the time derivative of the upper state population. We than divide the result by the number of incident photons per unit area per unit time, perform rotational averaging of the light field (remembering its vectorial nature), and obtain the absorption cross section:

$$\begin{aligned}\sigma(\omega_{\mathrm{I}}) &= \frac{8\pi\hbar\omega_{\mathrm{I}}}{{\epsilon_{\mathrm{I}}}^2 c}\frac{\mathrm{d}}{\mathrm{d}t}\langle\Psi^{(1)}(\boldsymbol{x},t)|\Psi^{(1)}(\boldsymbol{x},t)\rangle\\ &= \frac{2\pi\omega_{\mathrm{I}}}{3\hbar c}\int_{-\infty}^{\infty}\langle\Psi_i(\boldsymbol{x},-\infty)|\mu\mathrm{e}^{-iH_{\mathrm{b}}t/\hbar}\,\mu|\Psi_i(\boldsymbol{x},-\infty)\rangle\mathrm{e}^{i\tilde{\omega}t}\mathrm{d}t\end{aligned} \tag{64}$$

where ω_{I} is the frequency of the incident light and we defined $\tilde{\omega}=\frac{E_i}{\hbar}+\omega_{\mathrm{I}}$. If we consider a complete set of excited eigenfunctions, obtained, for example, as a solution of the unperturbed Hamiltonian, we can expand our total wavefunction in this set and insert in eqn (64), thus obtaining the popular energy frame formula for the electronic absorption (UV-vis) spectrum in the Franck–Condon regime:

$$\sigma(\omega_{\mathrm{I}})=\frac{4\pi^2\omega_{\mathrm{I}}}{3\hbar c}\sum_n|\langle\Psi_n|\mu|\Psi_i\rangle|^2\delta(\tilde{\omega}_{\mathrm{I}}-\omega_n) \tag{65}$$

Before we discuss the significance and interpretation of eqn (65), it is important to say that eqn (64) and (65) can be obtained from a different approach, called *linear response theory* (LRT).[5,7] In general, LRT is concerned with finding an approximation for the expectation value of an operator $\langle\Psi|\mathcal{A}|\Psi\rangle$ in the perturbative regime, if one considers only the first order in perturbation (thus, linear response). This is attained by expanding $\langle\Psi|\mathcal{A}|\Psi\rangle$ into a Taylor series in terms of the perturbation $\mathcal{H}_1$. Each term will be related to a different molecular property.

Downloaded from http://books.rsc.org/books/edited-volume/chapter-pdf/1851664/bk9781837676200-00271.pdf by University of Kent user on 28 January 2025

In the case of molecular absorption, the interaction of light with matter generates a dipole (polarization). In a general formulation, the polarization P will be expanded in a power series of the field strength ϵ. To linear approximation, we can keep the first term $P = \chi\epsilon$ only, where χ is the macroscopic susceptibility. In the microscopic level, this is related to the polarization $\langle\Psi|\mu|\Psi\rangle$. Expanding this in terms of the field perturbation, one can compare the terms to the expansion of Ψ and arrive at terms $P_{nm} = \langle\Psi^{(n)}|\mu|\Psi^{(m)}\rangle$, called coherences. If we consider the coherence $P_{01}(t) = \langle\Psi^{(0)}|\mu|\Psi^{(1)}\rangle$, using the definition of $\Psi^{(1)}$ (eqn (50)), we arrive at:

$$P_{01}(t) = \frac{i}{\hbar}\int_0^\infty \langle\Psi^{(0)}|\mu e^{-\frac{i\mathcal{H}_b t}{\hbar}}\mu|\Psi^{(0)}\rangle\epsilon(t-\tau)\mathrm{d}\tau \tag{66}$$

The quantity $C_{00}(t) = \langle\Psi^{(0)}|\mu e^{-\frac{i\mathcal{H}_b t}{\hbar}}\mu|\Psi^{(0)}\rangle$ is called the wavepacket correlation function. We see that $P_{01}(t)$ can be written as a convolution of $C_{00}(t)$ with a contribution of the field. $C_{00}(t)$ is the response function in this case. By applying a Fourier transform to eqn (66) and using the definition of the absorption spectrum, one can arrive at eqn (64) and (65).[5] With this formulation, we can thus interpret the absorption spectrum as the Fourier transform of the wavepacket correlation function.

Eqn (65) is the workhorse of one-photon spectroscopy calculations. This formulation of the excitation spectrum is sometimes referred to as the sum-over-states approach, since the summation in the formula runs through each of the eigenvectors of the reference wavefunction. The quantity under the summation is the average dynamic polarizability in the frequency space $\langle\alpha\rangle_\omega$ and is sometimes equivalently expressed as:[7,69]

$$\langle\alpha\rangle_\omega = \sum_n \frac{|\langle\Psi_n|\mu|\Psi_i\rangle|^2}{\tilde{\omega}_\mathrm{I} - \omega_n} \tag{67}$$

or

$$\langle\alpha\rangle_\omega = \sum_n \left\{\frac{|\langle\Psi_n|\mu|\Psi_i\rangle|^2}{\tilde{\omega}_\mathrm{I} - \omega_n} - \frac{|\langle\Psi_n|\mu|\Psi_i\rangle|^2}{\tilde{\omega}_\mathrm{I} + \omega_n}\right\} \tag{68}$$

From LRT, one can interpret the perturbative absorption spectrum as arising from the response of the dynamic polarizability of a system to the radiation field. The spectrum is obtained by finding the poles of the polarizability function, *i.e.* the points where $\tilde{\omega}_\mathrm{I} = \omega_n$, which makes the value of $\langle\alpha\rangle_\omega \to \infty$. In such points, the photon frequency is in "resonance" with the energy difference between states, resulting in electronic transition by absorption of the photon. The probability of each transition is proportional to the numerator $|\langle\Psi_n|\mu|\Psi_i\rangle|^2$—these matrix elements being the transition dipole moment—, and can be used in different measures (*e.g.* oscillator strength, Einstein coefficients, *etc.*) to calculate the intensity of the absorptions.[70] The result of such a calculation is a stick-like spectrum with positive amplitudes at each absorption frequency. These are called vertical or Frank–Condon excitations, and do not consider the vibrational levels, which one can include by adding vibrational Hamiltonian matrix elements in the formulation.[68] The vibronic coupling accounts for most of the band shape in electronic spectra. The temperature and solvent

Downloaded from http://books.rsc.org/books/edited-volume/chapter-pdf/1851664/bk9781837676200-00271.pdf by University of Kent user on 28 January 2025

polarization are also contributors and can be included through a variety of approaches, although it is not straightforward.[71–85]

To apply the polarizability-based approach above, one only needs to know the set of ground and excited states wavefunctions. We recall once again that such an approach carries all the usual problems related to the choice of the reference wavefunction, and a complete set of Ψ_n is unattainable, demanding the use of an approximate basis set. LRT (or RPA) approaches are available in most software packages applied to a variety of electronic models such as HF, DFT, VB, CI, and CASSCF. LRT applied to CC methods are possible (*e.g.* LR-CC2), but the expressions derived in this section are not suitable for non-variational wavefunctions. The poles of the polarizability matrix are still a measure of excitation energies in such cases, but the expression must be formulated in terms of the derivative of the action Lagrangian (shown below). LR-CC formulations suffer from many problems, including lack of size extensivity and consistency. Notice that this procedure is primarily meant to obtain frequencies and intensities of transitions (properties), rather than attaining to calculate the wavefunctions and excited state dynamics, although some qualitative characterisation of the wavefunctions is possible through the consideration of the transition dipole moments.

2.4 Variational methods

The TDPT formalism above relies on an imperfect reference, in the sense that no exact solution to the unperturbed wavefunction exists. A variational theory of the TDSE is, in principle, exact and offers a more reliable way of approximating the time-dependent wavefunction and property calculations. Many possible formulations exist depending on the choice of parameters and approximation schemes. Many variational approaches are so-called *local in time*. This means that the wavefunction at a time $t' = t + \Delta t$ is variationally optimised taking the wavefunction at t as a reference. The reference can only be exact when $t = 0$, which is the ground state stationary wavefunction $\Psi(x,0)$. Variational formulations that are global in time are possible through numerical methods.

The main working equation of a variational formulation for the TDSE is a stationary condition to the action integral defined as:

$$S[\Psi] = \int_{t_0}^{t} \left\langle \Psi \middle| i\frac{\partial}{\partial t} - \mathcal{H} \middle| \Psi \right\rangle \mathrm{d}t' \tag{69}$$

Given a wavefunction *ansatz*, the variation δS of this action is minimised to obtain the optimised variational wavefunction. By an analogous approach to the HF method, one can build a time-dependent Fock operator with time-dependent orbitals and energies as solutions and construct a time-dependent SCF framework to optimise the (time-dependent) orbital coefficients in a finite atomic basis set.[5,7] Naturally, this approach can be extended to all post-HF methods as well as to VB methods. A similar approach can be used to derive time-dependent Kohn–Sham equations in the TDDFT approach.[7,86] In general, for absorption spectroscopy, LRT will be applied for the calculation of excitation energies and properties, arriving at the usual eqn (64) and (65).

Downloaded from http://books.rsc.org/books/edited-volume/chapter-pdf/1851664/bk9781837676200-00271.pdf by University of Kent user on 28 January 2025

2.5 Propagators and equation-of-motion methods

We have come across the definition of an evolution operator or propagator above, as an operator which maps $\Psi(\boldsymbol{x},t=0)\rightarrow\Psi(\boldsymbol{x},t)$. After defining our perturbed Hamiltonian for light–matter interaction, we arrived at an expression which maps a wavefunction $\Psi_i(\boldsymbol{x},-\infty)$ into the first order correction to the wavefunction $\Psi^{(1)}(\boldsymbol{x},t)$ (eqn (63)). The quantity multiplying $\Psi_i(\boldsymbol{x},-\infty)$ is, therefore, a propagator. When discussing LRT, we have seen that this quantity leads to the correlation function, whose Fourier transform can be interpreted as the absorption spectrum. Furthermore, we have seen that this is equivalent to the response of the average polarizability in the frequency domain $\langle\alpha\rangle_\omega$ plus constants. From this, we can see that there is a close connection between the properties of a propagator and time-dependent molecular properties such as the polarizability, which leads to excitation energies. Writing the TDSE in the Heisenberg picture, one can in fact work directly with propagators, without any need to consider expansions of the time-dependent wavefunction. If we Taylor-expand the expectation value of the dipole moment operator $\langle\Psi|\mu|\Psi\rangle$ in terms of the perturbation H_1 as defined in eqn (61), we arrive at a propagator-based expansion. It can be shown that the first order term is the frequency dependent polarizability which we are already familiar with. Propagators can be used in a broader way for a variety of time-dependent formulations, going beyond perturbation theory or variational approximations and even considering QFT formulations. For this, one considers the calculation of the general propagators as solution to their equation-of-motion (*e.g.* eqn (54)), thus avoiding the costly calculation of corrections to the wavefunction. In this context it is common to call the propagators Green's functions, since they are essentially the solutions to differential equations involving a linear differential operator.[87] Such a treatment is beyond the scope of this text, but ref. 5, 7 and 69 discuss some propagator approaches in more detail.

A different approach to the calculation of excited states is what is conventionally called *equation-of-motion* (EOM) methods. In this approach, one starts from the assumption that an excited state wavefunction Ψ_n is produced from the ground-state wavefunction Ψ_0 by an excitation operator $\mathcal{O}_n^\dagger$ (with a corresponding de-excitation operator $\mathcal{O}_n$). Defining a Hamiltonian superoperator $\widehat{\mathcal{H}}$, or Liouvillian, as an object that, when operating on an operator $\mathcal{A}$, generates the commutator with the Hamiltonian:

$$\widehat{\mathcal{H}}\mathcal{A}=[\mathcal{H},\mathcal{A}] \tag{70}$$

one can see that, for exact state eigenfunctions, we have:

$$\widehat{\mathcal{H}}\mathcal{O}_n^\dagger|\Psi_0\rangle=\mathcal{H}\mathcal{O}_n^\dagger|\Psi_0\rangle-\mathcal{O}_n^\dagger\mathcal{H}|\Psi_0\rangle=(E_n-E_0)\mathcal{O}_n^\dagger|\Psi_0\rangle \tag{71}$$

Thus, when acting on the exact ground state wavefunction, $\widehat{\mathcal{H}}\mathcal{O}_n^\dagger$ returns the excitation energy. Therefore, $\mathcal{O}_n^\dagger$ is an eigenoperator of $\widehat{\mathcal{H}}$ with eigenvalue equal to the exact excitation energy. By seeking (approximate) solutions to the eigenvalue equation above, *e.g.* by using an operator basis to expand $\mathcal{O}_n^\dagger$, one can formulate a general theory based on these

Downloaded from http://books.rsc.org/books/edited-volume/chapter-pdf/1851664/bk9781837676200-00271.pdf by University of Kent user on 28 January 2025

quantities and calculate excitation energies without the need to bother about approximations to the time-dependent wavefunction. Although no explicit mention of the equation-of-motion was made, the commutation relations arising from such formulations resemble those found when applying the equation-of-motion to operators in the Heisenberg picture, as discussed in the paragraph above.[69]

Recall that, when discussing ΔSCF methods, we argued that CC wavefunctions are not suitable due to their HF reference. The EOM technique can be applied to CC wavefunctions with a suitable expansion of the excitation operators $\mathcal{O}_n^\dagger$ for a given cluster exponential operator. This is generally done by a similarity transform of the Hamiltonian such that it commutes with the approximate $\mathcal{O}_n^\dagger$ operator. To perform this, a CIS matrix is used as an initial guess for the singles and doubles space Hamiltonian. Currently, EOM-CCSD is the highest level of this approach since reliable implementations for EOM-CCSD(T) or EOM-CCSDT have not been developed.

EOM-CC methods are costly, but an alternative similarity transformed EOM (STEOM) approach exists.[88] In this version, a second similarity transform to the Hamiltonian further compresses the space to the CIS space only, thus decreasing the cost. Multireference formulations of this approach are also available. A word of caution regarding these methods is that they are not size consistent or extensive.

Except for the CC method discussed above, when applied to other reference wavefunctions at the usual level of approximation considered here, EOM, propagator, perturbative and variational methods all lead to the same working equations for discussing electronic excitations. For example, with a one-determinant closed-shell reference function and a single excitation manifold, all methods yield the standard LRT (or RPA) equations.[69]

2.6 Algebraic diagrammatic construction methods

The last class of methods to be discussed is the so called *algebraic diagrammatic construction* (ADC) methods, amongst which the most popular approach is ADC(2).[89] These methods can effectively include correlation to the excited states through perturbative methods at a considerably lower cost than the CI or CC approaches discussed above. The origin of ADC methods lies in the propagators or Green's function approach briefly discussed above, but current developments rely on the Liouvillian formalism similar to EOM methods.

Originally, for electronic transitions, the ADC method involved expanding the polarizability propagator in the perturbative regime in terms of diagrammatic perturbation theory. The MP partitioning of the Hamiltonian (Section 1.5) is used to construct the wavefunctions, and the perturbative order n to which this is carried out determines the ADC(n) level.

Because of this, such methods include correlation, but are not suitable for multireference systems, of which organometallic systems are an example. Only excitation properties and energies are available through this

Downloaded from http://books.rsc.org/books/edited-volume/chapter-pdf/1851664/bk9781837676200-00271.pdf by University of Kent user on 28 January 2025

formulation, with no excited state wavefunction obtained. However, by using representations of the propagators (known as intermediate states representation), akin to what is obtained by the EOM approach, the ADC matrices can be built and used to calculate approximate wavefunctions. These representations, from ADC(2) onward, are also correlated references. ADC(2) offers good quality excitation spectra, comparable to the EOM-CCSD approach, but with a cheaper and easier implementation. For more details, see ref. 90.

One limitation of ADC lies in its single-reference framework, which restricts its applicability to systems exhibiting open-shell or multireference characters in their ground or excited electronic states. A comprehensive multireference ADC (MR-ADC) formulation has been proposed by Sokolov,[91] achieved by integrating the Liouvillian formalism with MRPT. This formulation extends the conventional ADC theory to accommodate multiconfigurational reference wavefunctions. MR-ADC methods are comparable in computational expense to low-order multireference perturbation theories and are capable of calculating various electronic spectra, including UV-Vis, X-ray absorption, and UV/X-ray photoelectron spectra. MR-ADC calculations were, however, restricted to small molecules due to their inefficient spin–orbital implementation. Recent advancements by de Moura and Sokolov,[92] incorporating spin adaptation, density fitting, and automated code generation, promise to significantly enhance the efficiency of MR-ADC, potentially enabling calculations for systems with over 1500 molecular orbitals. A newly reported application of this improved MR-ADC methodology in organometallic chemistry involves the analysis of X-ray photoelectron spectra of $Fe(CO)_5$ and its photodissociation products ($Fe(CO)_4$, $Fe(CO)_3$) after excitation with 266 nm light (Fig. 2).[93] These calculations indicated that core-hole screening, spin–orbit coupling, and ligand-field splitting are all crucial factors in accurately reproducing the experimentally observed chemical shifts in the transient Fe 3p XPS spectra of iron carbonyl complexes.

3 Some applications in organometallic chemistry

The popularity of TDDFT methods for excited states cannot be overstated. Their ease of use even by non-experts, wide availability, and capacity of accounting for a major part of correlation effects at a fractional cost compared to post-HF methods make for a highly attractive method. This became clear in a 2010 survey, where, according to the statistics of the papers published from 2007 to 2010 in the field of excited states, the use of different methods is distributed as follows: TDDFT: 50%, single-configuration methods: 23%, and multiconfigurational methods: 26%.[94,95] Another, slightly more recent, survey shows a similar distribution with a more refined classification.[96] Other important reviews in the field address a range of methods and exemplary organometallic systems such as: (1) interpretation and accuracy of electronic absorption spectra, treatment of long-range charge transfer states and spin–orbit coupling effects, environmental effects, and dynamical and QM/MM methods;[97] (2) binary

Downloaded from http://books.rsc.org/books/edited-volume/chapter-pdf/1851664/bk9781837676200-00271.pdf by University of Kent user on 28 January 2025

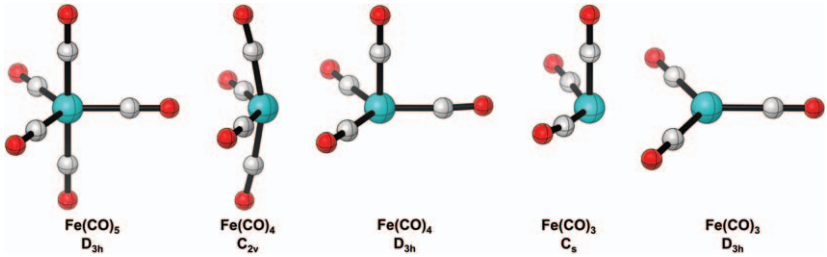


Fig. 2 Iron carbonyl complexes investigated by Gaba *et al.*,[93] together with their point-group symmetries. All systems are depicted in their singlet states.

metal carbonyl photodissociation, non-adiabatic relaxation, Jahn–Teller and pseudo-Jahn–Teller effects, photoisomerization of transition metal complexes, and coupled cluster response theory for electronic spectroscopy;[98] (3) excited state dynamics of transition metal complexes, from the wavefunction to the dynamical level.[99]

Despite the advantages and the remarkable success of DFT, we have repeatedly emphasized in this text the many flaws of this method. We have highlighted the necessity of benchmarking and carefully assessing the quality of the results obtained against higher quality computational methods and experiment. This is not a trivial task, and much is yet to be done, but the following examples demonstrate progress in this area. Latouche *et al.*[100] benchmark DFT functionals and ECP basis sets against experimental data for absorption energies of Pt(II) and Ir(III) complexes (Fig. 3a). Paranthaman *et al.*[101] investigate the performance of DFT and relativistic ECP for Ru-based organometallic complexes (Fig. 3b). Garino & Salassa[102] review DFT and TDDFT methods for a variety of photochemically active organometallic compounds. Harvey[103] critically evaluates the use of DFT to treat transition metal chemistry in general. Niehaus *et al.*[104] investigate the TDDFT description of charge transfer excited states, using a series of 17 pseudo-square planar platinum(II) and pseudo-octahedral iridium(III) complexes (Fig. 3c) that are known to feature quite different localization characteristics ranging from ligand-centred (LC) to metal-to-ligand charge transfer (MLCT) transitions. Maschietto *et al.*[105] call attention to the existence of spurious low-lying excited states from TDDFT and offer a methodology to address the problem.

Two recent examples illustrate interesting contrasts between TDDFT and multiconfiguration methods. In the first, Costa *et al.*[106] compare TDDFT and CASSCF/MS-CASPT2 applied to the description of excited states for the complex $(CH_3)ReO_3$ (Fig. 3d). Although both methods yield similar energies, a small difference in the characterisation of the second transition exists. This is a charge transfer from C and O to Re, but the participation of C, as described by CASSCF/MS-CASPT2, is much smaller than described by TDDFT. In their studies, the authors utilised the LB94 functional, which tries to correct for the wrong DFT asymptotic behaviour, but is found to be the worst amongst the tested functionals in describing the excitation energies.[106] In the second study, Escudero *et al.*[107] compared RASPT2/RASSCF to range-separated/hybrid DFT

Downloaded from http://books.rsc.org/books/edited-volume/chapter-pdf/1851664/bk9781837676200-00271.pdf by University of Kent user on 28 January 2025

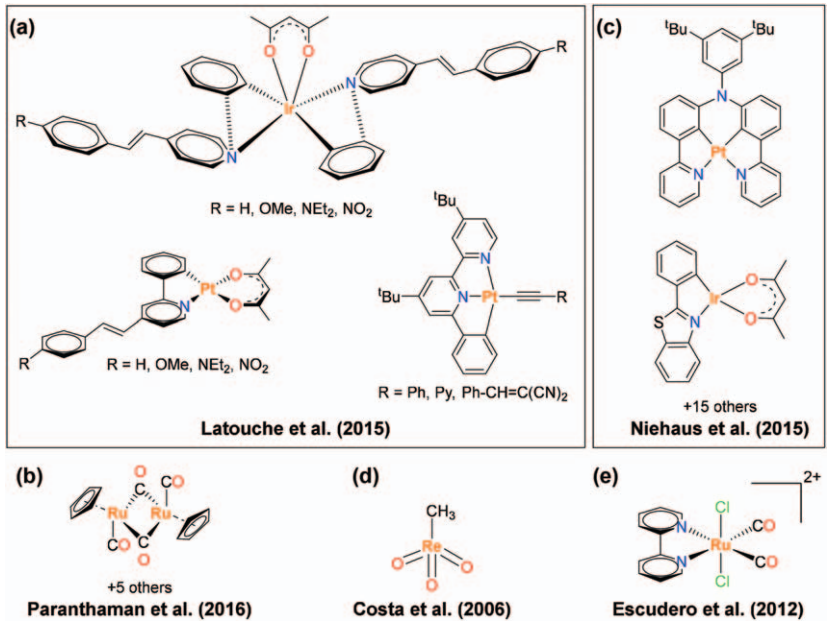


Fig. 3 Metal complexes mentioned in Section 3.

methods in excited states of the Ru(II) bipyridyl complex *trans*(Cl)-Ru(bpy)-$Cl_2(CO)_2$ (bpy = bypyridyl, Fig. 3e). The authors discuss the difficulty in partitioning the RAS subspaces, and benchmark various types of TDDFT functionals including implicit solvent models. It is found that none of the functionals can optimally describe all the excited states simultaneously. However, the hybrid M06, B3LYP, and PBE0 functionals seem to be the best compromise to obtain a balanced description of the excited states of *trans*(Cl)-Ru(bpy)$Cl_2(CO)_2$, when comparing with the experimental spectrum.[107]

Below, we will consider further applications and more critical assessment of DFT and multireference methods in different contexts. The intention is to highlight some of the complexities, successes, and challenges in different fields.

3.1 Spin-crossover materials and photodevices

Spin-crossover (SCO) materials[108,109] are a fascinating area of research in organometallic chemistry, particularly in the context of first-row transition metals, where the electronic spin state can be reversibly switched between high-spin and low-spin configurations by external stimuli. Accurate prediction and understanding of SCO behaviour is crucial for the development of novel materials with potential applications in sensors and displays. Computational methods, in particular TDDFT and CASSCF/CASPT2, play a central role in these investigations. For example, Phung *et al.*[110] have shown that a combined CASPT2/CC approach, using high-quality CASPT2 with extensive correlation-consistent basis sets for valence correlation and low-cost CCSD(T) calculations with minimal basis sets, is efficient for spin-state energetics of a series of iron complexes

Downloaded from http://books.rsc.org/books/edited-volume/chapter-pdf/1851664/bk9781837676200-00271.pdf by University of Kent user on 28 January 2025

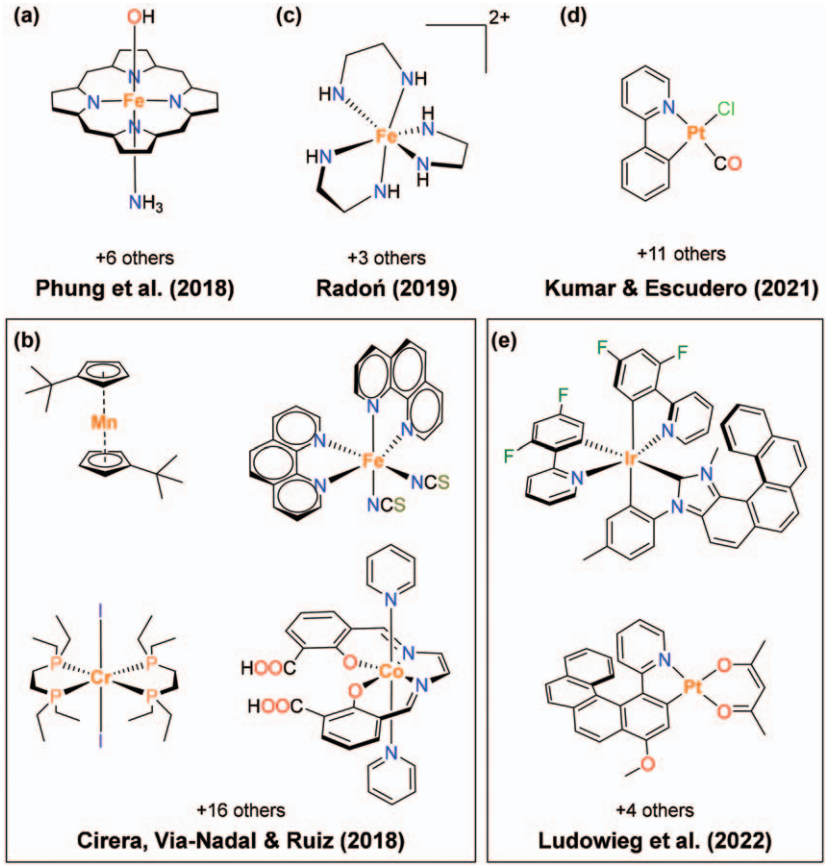


Fig. 4 Metal complexes mentioned in Section 3.1.

(Fig. 4a), with errors estimated to be around 2 kcal mol^{-1} in favour of the high spin states. Reimann & Kaupp[111] used another composite method, the CASPT2+δMRCI method, to calculate the SCO energy. For a series of $[Fe(He)_6]^{n+}$ test complexes, the approach reproduces the full MRCISD+Q/CBS results with an accuracy of less than 0.04 eV. Cirera, Via-Nadal, & Ruiz[112] presented a systematic study on the performance of different density functional methods to study SCO on first-row transition metal complexes (Fig. 4b). Amongst the tested functionals, the hybrid meta-GGA functional TPSSh with a triple-ζ basis set containing polarization functions for all atoms gives the best results for different metals and oxidation states, and its performance in predicting the correct ground state and energy window for the occurrence of SCO is quite satisfactory. Radoń[113] also performed advanced benchmark studies showing, for example, that NEVPT2 performs worse than CASPT2, and that the double hybrid B2PLYP-D3 is able to provide a balanced description of spin state energies for the four studied iron complexes simultaneously (Fig. 4c). Such examples illustrate the continuous refinement of computational methods to better capture the complex phenomena underlying SCO processes.

Downloaded from http://books.rsc.org/books/edited-volume/chapter-pdf/1851664/bk9781837676200-00271.pdf by University of Kent user on 28 January 2025

Transitioning from SCO materials to photodevices, computational studies have provided important insights for the development of materials with optimal light emission properties. In the field of phosphorescent materials, which are central to the next generation of organic light emitting diodes (OLEDs), understanding the photophysics and relative position of the lowest energy triplet excitation, T_1, is crucial and has therefore been recently reviewed in various contexts. For example, Powell[114] has reviewed theories of phosphorescence in cyclometallated complexes, highlighting the crucial role of both scalar relativistic effects and spin–orbit coupling in accurately modelling the phosphorescent properties. These effects, incorporated *via* TDDFT, provide quantitatively accurate predictions of radiative decay rates, which are crucial for the development of effective photodevices. Kumar & Escudero,[115] in turn, used *domain-based local pair natural orbital* CC Theory (DLPNO-CCSD(T)) to calculate the phosphorescence energies of a variety of Pt(II) complexes (Fig. 4d) with potential application as components in phosphorescent organic light-emitting diodes (PhOLEDs). This approach, which included a rigorous test of various relativistic effects and a comparison of several DFT functionals, revealed that M06HF performed the best. Finally, Ludowieg *et al.*[116] focused on the calculation of magnetic transition dipole moments and rotational strengths using the relativistic two-component TDDFT with ZORA. This approach was applied to evaluate the phosphorescence dissymmetry factors and lifetimes of iridium complexes based on N-heterocyclic carbenes and platinum helicenes (Fig. 4e), showing excellent agreement with experimental data.

3.2 Imaging in life sciences

Organometallic compounds have traditionally been celebrated for their catalytic ability, yet their potential in the realm of chemical biology, including for bioimaging applications, is increasingly being recognised.[117] Despite initial reservations about their stability and cytotoxicity under physiological conditions, many compounds are proving to be invaluable due to their unique physicochemical properties such as robust chemical stability, structural diversity, and distinct photo- and electrochemical behaviours.

One of the most noteworthy developments in the bioimaging area is the use of BODIPY (4,4-difluoro-4-bora-3*a*,4*a*-diaza-*s*-indacene) fluorophores (Fig. 5a),[118] renowned for their high brightness and exceptional chemical and photochemical stability. Recent advancements have seen BODIPY derivatives being engineered to serve as multimodal imaging probes, theranostic agents, and sensitisers for photodynamic therapy. The adaptability of BODIPY synthesis allows for the creation of metal-based BODIPY derivatives tailored for medical applications, merging the luminescent properties of BODIPY with the therapeutic or diagnostic functions of metal complexes. This synthesis strategy has led to the design of compounds that not only act as potent cytotoxic agents but also facilitate real-time tracking of their biodistribution and mechanism of action *in vivo*, enhancing the understanding of their biological interactions.

Downloaded from http://books.rsc.org/books/edited-volume/chapter-pdf/1851664/bk9781837676200-00271.pdf by University of Kent user on 28 January 2025

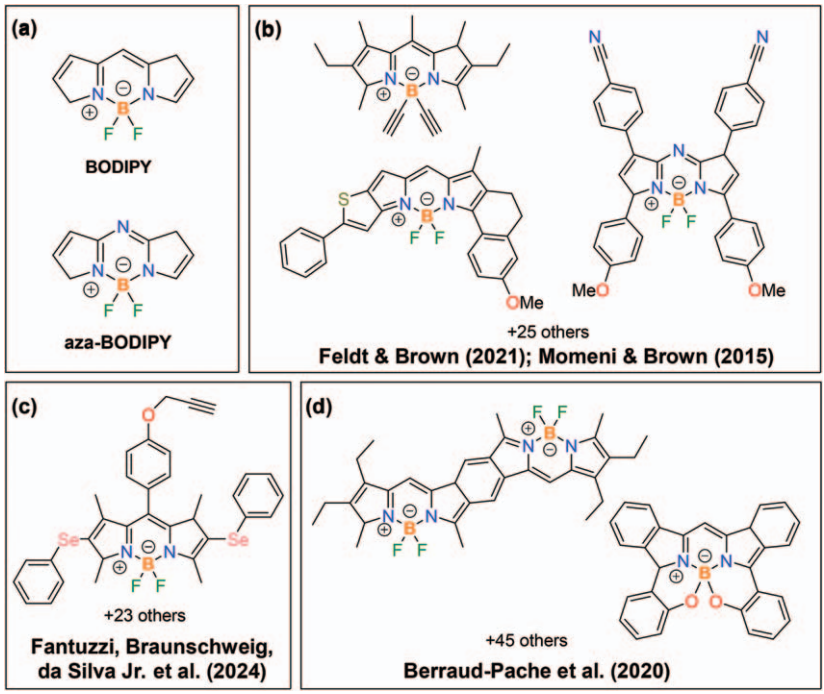


Fig. 5 BODIPY and aza-BODIPY core plus derivative molecules mentioned Section 3.2.

From a computational standpoint, accurately modelling the intricate structures of organometallic compounds and their interactions within biological systems is vital for predicting their performance and refining their design. Recent studies, such as those by Feldt & Brown,[119] have utilised local CC methods to compute vertical excitation energies for a benchmark set of seventeen BODIPY/aza-BODIPY molecules, comparing these computational predictions with experimental results (Fig. 5b). These studies demonstrated that methods like DLPNO-STEOM-CCSD offer excellent correlation with experiments, making it one of the most accurate single-reference methods available. Similarly, Momeni & Brown[120] (Fig. 5b) conducted benchmark studies using TDDFT, revealing that the approach faces challenges related to handling differential electron correlation and the impacts of multireference character and double excitations, which contribute to discrepancies in computational accuracy.

Recently, in collaboration with the groups of Braunschweig & da Silva Jr., we have developed a novel method for the late-stage electrochemical diselenation of BODIPYs (Fig. 5c),[121] revealing red-shifted absorption and tuneable colour emission with substantial Stokes shifts in selenium-containing derivatives. Photophysical analyses, supported by TDDFT and DLPNO-STEOM-CCSD computations, showed that DLPNO-STEOM-CCSD aligns closer with experimental results than TDDFT, although TDDFT better captures energy differences due to cancellation of errors and lack of size consistency of the CC approach. The selenium-containing BODIPYs notably demonstrate selective staining of lipid droplets with distinct fluorescence, highlighting their potential in bioimaging applications.

Downloaded from http://books.rsc.org/books/edited-volume/chapter-pdf/1851664/bk9781837676200-00271.pdf by University of Kent user on 28 January 2025

Postils, Ruipérez & Casanova,[122] in turn, rationalised the electronic structure of BODIPYs by combining a variety of quantum chemical methods and computational tools. They showed that BODIPYs have a mild open-shell character, which explains the usual failure of TDDFT methods. By comparing a large number of methods, the authors concluded that the $S_0 \rightarrow T_1$ transition energies are significantly improved by using methods with double excitation effects, including post-HF, and single-reference correlation methods such as ADC(2). Finally, Berraud-Pache *et al.*[123] used DLPNO-STEOM-CCSD to calculate the lowest vertical excitation energies of more than 50 BODIPY molecules (Fig. 5d). The method worked remarkably well, providing an accuracy of about 0.06 eV compared to the experimental data. These examples show that the DLPNO-STEOM-CCSD method is appropriate for studying the photophysical properties of medium to large organic compounds. The results also emphasise the complexity of computational approaches and highlight the need for continued refinement of these methods to improve prediction accuracy.

3.3 Nanofabrication

Nanofabrication and metallisation of organic thin films have diverse applications in fields such as energy harvesting, electronics, and sensing. Two central experimental techniques in this domain include photo-assisted chemical vapour deposition (PACVD)[124–126] and focused electron beam induced deposition (FEBID).[127] PACVD utilises photoinduced reactions to initiate the decomposition of organometallic precursors, offering a viable method for metallising organic films at or near room temperature. Conversely, FEBID enables the creation of 3D metallic structures with sub-10 nm dimensions on both planar and nonplanar surfaces. In this process, metal-containing precursor molecules are physisorbed on a substrate and degraded by a focused high-energy electron beam to yield a metallic deposit.

A critical aspect in the effectiveness of these nanofabrication techniques is the selection of suitable organometallic precursors. From a theoretical perspective, understanding the photoabsorption spectra and the dynamics of excited states following ligand dissociation is essential. Theoretical studies, particularly employing TDDFT, have been instrumental in elucidating these aspects. For instance, Walker, McElwee-White *et al.*[124,125] have extensively studied the photoabsorption spectra of ruthenium carbonyl complexes featuring either η^4 (Fig. 6a) or η^3 (Fig. 6b) ligands. Their studies utilised hybrid functionals to characterise excited states, assigned, *e.g.* as metal-to-ligand charge transfer or ligand-field states. Similarly, Zlatar, Allan, & Fedor[127] have utilised TDDFT calculations integrated with ZORA to analyse tetrakis(trifluorophosphine)platinum(0), $Pt(PF_3)_4$, a model precursor for FEBID (Fig. 6c). Their studies not only validated the computed electronically excited states up to 13 eV through comparison with electron energy loss spectra, but also explored potential energy curves for these states. They demonstrated that the lowest excited states are either directly dissociative or proceed *via* conical

Downloaded from http://books.rsc.org/books/edited-volume/chapter-pdf/1851664/bk9781837676200-00271.pdf by University of Kent user on 28 January 2025

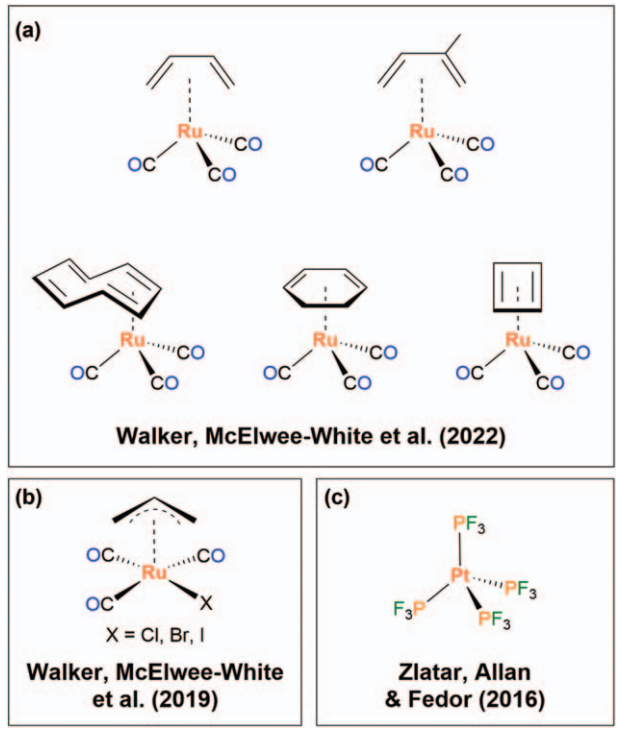


Fig. 6 Ruthenium and platinum precursors mentioned in Section 3.3.

intersections, facilitating dissociation pathways. Their findings underscored the predominance of the neutral dissociation channel over dissociative electron attachment for $Pt(PF_3)_4$, a conclusion that may also extend to other FEBID precursors.

3.4 Artificial photosynthesis

Artificial photosynthesis is a technology that replicates natural photosynthesis by using sunlight to split water into oxygen, protons, and electrons; these electrons can then be used to reduce protons or carbon dioxide (CO_2) into energy-dense fuels like hydrogen or hydrocarbons. It aims to provide a sustainable energy solution by converting solar energy into chemical fuels, addressing the rising global energy demand and costs associated with finite conventional fuels.[128,129]

The integration of computer-aided design with synthesis and spectroscopic characterisation has significantly advanced the development of artificial photosynthetic systems. The employment of semiconductor electrodes that are modified through the covalent attachment of molecular dyes enhances visible light absorption. Computational modelling has proven indispensable in formulating sensitisers and anchoring groups robust enough to operate under aqueous and oxidative conditions, facilitating rapid electron transfer at the interfaces. Wavefunction-based methods, including EOM-CCSD, CASSCF, CASPT2, NEVPT2, and MRCI, are increasingly being utilized in this field. For instance,

Downloaded from http://books.rsc.org/books/edited-volume/chapter-pdf/1851664/bk9781837676200-00271.pdf by University of Kent user on 28 January 2025

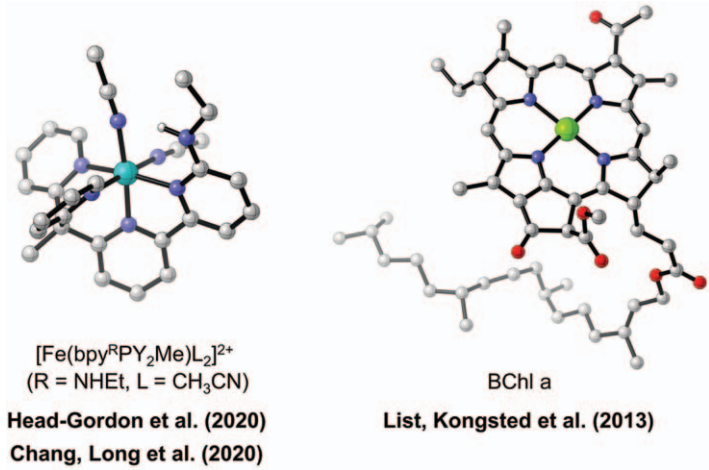


Fig. 7 Examples of organometallic systems relevant to light-harvesting applications. For the iron complex, bpy^{R}PY$_2$Me = 6-(1,1-bis(pyridin-2-yl)ethyl)-2,2′-bipyridine; NHEt = ethylamine. All H atoms pertaining to C–H bonds are omitted for clarity.

Head-Gordon *et al.*[130] computationally investigated an iron(II) polypyridine electrocatalyst (Fig. 7a) for the conversion of CO_2 to carbon monoxide, a complex synthesized by Chang, Long *et al.*[131] They specifically used CASSCF/NEVPT2 calculations to obtain static and dynamic correlations, determining the energy differences between isomers of a doubly reduced intermediate in the reaction.[130] Additionally, List, Kongsted *et al.*[132] examined the efficacy of various single-reference methods for assessing pigment–protein complexes, specifically in predicting the relative site energies and transition moments of the Q bands in the bacteriochlorophyll a (BChl a) pigments of the Fenna–Matthew–Olson (FMO) complex, comparing these against a hybrid DFT/MRCI approach (Fig. 7b).

Naturally, the computational demands of these methods restrict their use primarily to benchmark smaller molecular models. As a more cost-effective alternative, TDDFT is extensively utilised in artificial photosynthesis and the calculation of absorption spectra of dyes and nanoclusters. To enhance the accuracy, especially for charge-transfer excitations, sophisticated functionals such as range-separated hybrid functionals have been developed, showing considerable promise in improving predictive performance in the field.

4 Final remarks

In this chapter, we have explored a comprehensive array of quantum mechanical methods for modelling excited states in organometallic chemistry. The landscape of computational strategies is vast and nuanced, requiring a thorough understanding of each method's theoretical foundations and practical applications. From fundamental wavefunction methods like Hartree–Fock, configuration interaction, and coupled-cluster to the more computationally efficient density functional theory

Downloaded from http://books.rsc.org/books/edited-volume/chapter-pdf/1851664/bk9781837676200-00271.pdf by University of Kent user on 28 January 2025

and its time-dependent variants, each approach has its strengths and limitations. We discussed the intricacies of perturbative methods, multireference approaches, and the importance of considering relativistic effects, especially for systems involving heavy atoms. Valence bond methods, while less common in organometallic contexts, provide an alternative perspective aligned with the chemist's traditional view of chemical bonding. The chapter also highlighted the challenges and advances in excited state calculations, emphasising the need for appropriate method selection to balance computational cost and accuracy. Techniques such as the ΔSCF approach, time-dependent perturbation theory, and the equation-of-motion methods offer robust frameworks for studying dynamic properties and interactions of molecular systems with light. Furthermore, we discussed several applications of these theoretical approaches in the field of organometallic chemistry. Particular focus was given to the theoretical description of organometallics in various contexts, including spin-crossover materials and photodevices, bioimaging, nanofabrication, and artificial photosynthesis. Overall, we have provided a detailed roadmap for understanding and applying computational methods to model excited states in organometallic systems. As computational resources and algorithms continue to advance, the accuracy and applicability of these methods will only improve, opening new frontiers in chemical research and industrial applications.

Acknowledgements

This work was supported by the Engineering and Physical Sciences Research Council [grant number EP/W52461X/1]. We also acknowledge the University of Kent for their financial support. The authors are grateful for partial financial support by the European Commission through the RADON project (GA 872494) within the H2020-MSCA-RISE-2019 call. This chapter is based on work from the COST Action CA20129 – Multiscale Irradiation and Chemistry Driven Processes and Related Technologies (MultIChem), supported by COST (European Cooperation in Science and Technology).

References

1 I. N. Levine, *Quantum Chemistry*, Pearson, Upper Saddle River, 7th edn, 2014.
2 M. Persico and G. Granucci, *Photochemistry*, Springer International Publishing, Cham, 2018.
3 G. A. Worth and L. S. Cederbaum, *Annu. Rev. Phys. Chem.*, 2004, **55**, 127–158.
4 T. F. O'Malley, in *Advances in Atomic and Molecular Physics*, 1971, vol. 7, pp. 223–249.
5 D. Tannor, *Introduction to quantum mechanics: a time-dependent perspective*, University Science, Sausalito, 2007.
6 A. Szabó and N. S. Ostlund, *Modern Quantum Chemistry*, Dover Publications, Mineola, 1989.
7 F. Jensen, *Introduction to Computational Chemistry*, John Wiley & Sons, Ltd, Chichester, 3rd edn, 2017.
8 A. V. Sergeev and D. Z. Goodson, *J. Chem. Phys.*, 2006, **124**, 094111.

Downloaded from http://books.rsc.org/books/edited-volume/chapter-pdf/1851664/bk9781837676200-00271.pdf by University of Kent user on 28 January 2025

9 J. Olsen, P. Jørgensen, T. Helgaker and O. Christiansen, *J. Chem. Phys.*, 2000, **112**, 9736–9748.
10 C. Angeli, R. Cimiraglia, S. Evangelisti, T. Leininger and J.-P. Malrieu, *J. Chem. Phys.*, 2001, **114**, 10252–10264.
11 C. Angeli, R. Cimiraglia and J.-P. Malrieu, *Chem. Phys. Lett.*, 2001, **350**, 297–305.
12 C. Angeli, R. Cimiraglia and J.-P. Malrieu, *J. Chem. Phys.*, 2002, **117**, 9138–9153.
13 S. Chattopadhyay, R. K. Chaudhuri, U. S. Mahapatra, A. Ghosh and S. S. Ray, *Wiley Interdiscip. Rev.: Comput. Mol. Sci.*, 2016, **6**, 266–291.
14 E. A. Hylleraas, *Z. Phys.*, 1929, **54**, 347–366.
15 L. Kong, F. A. Bischoff and E. F. Valeev, *Chem. Rev.*, 2012, **112**, 75–107.
16 S. Ten-no and J. Noga, *Wiley Interdiscip. Rev.: Comput. Mol. Sci.*, 2012, **2**, 114–125.
17 G. N. Lewis, *J. Am. Chem. Soc.*, 1916, **38**, 762–785.
18 G. N. Lewis, *Valence and the structure of atoms and molecules*, Chemical Catalog, 1923.
19 L. Zhao, W. H. E. Schwarz and G. Frenking, *Nat. Rev. Chem.*, 2019, **3**, 35–47.
20 X. Lin and Y. Mo, *Inorg. Chem.*, 2022, **61**, 2892–2902.
21 S. Đorđević, S. Radenković, S. Shaik and B. Braïda, *Molecules*, 2022, **27**, 490.
22 J. Li, Q. Feng, C. Wang and Y. Mo, *Phys. Chem. Chem. Phys.*, 2023, **25**, 15371–15381.
23 J. Joy, D. Danovich, M. Kaupp and S. Shaik, *J. Am. Chem. Soc.*, 2020, **142**, 12277–12287.
24 M. A. S. Francisco, F. Fantuzzi, T. M. Cardozo, P. M. Esteves, B. Engels and R. R. Oliveira, *Chem. – Eur. J.*, 2021, **27**, 12126–12136.
25 D. W. O. de Sousa and M. A. C. Nascimento, *J. Chem. Phys.*, 2022, **157**, 174302.
26 R. Pauncz, *The symmetric group in quantum chemistry*, CRC Press, Boca Raton, 1995.
27 R. Pauncz, *Spin eigenfunctions: construction and use*, Plenum Press, New York, 1979.
28 H. Weyl, *The theory of groups and quantum mechanics*, Dover, London, 1950.
29 M. Hamermesh, *Group theory and its application to physical problems*, Addison-Wesley Pub. Co, Reading, Mass, 1962.
30 W. Heitler and F. London, *Z. Phys.*, 1927, **44**, 455–472.
31 J. Gerratt, in *Advances in Atomic and Molecular Physics*, 1971, pp. 141–221.
32 J. Gerratt and W. N. Lipscomb, *Proc. Natl. Acad. Sci. U. S. A.*, 1968, **59**, 332–335.
33 J. Gerratt, D. L. Cooper, P. B. Karadakov and M. Raimondi, *Chem. Soc. Rev.*, 1997, **26**, 87.
34 R. C. Ladner and W. A. Goddard, *J. Chem. Phys.*, 1969, **51**, 1073–1087.
35 W. A. Goddard and L. B. Harding, *Annu. Rev. Phys. Chem.*, 1978, **29**, 363–396.
36 M. M. Goodgame and W. A. Goddard, *Phys. Rev. Lett.*, 1985, **54**, 661–664.
37 W. J. Hunt, P. J. Hay and W. A. Goddard, *J. Chem. Phys.*, 1972, **57**, 738–748.
38 W. A. Goddard, T. H. Dunning, W. J. Hunt and P. J. Hay, *Acc. Chem. Res.*, 1973, **6**, 368–376.
39 T. H. Dunning, L. T. Xu, D. L. Cooper and P. B. Karadakov, *J. Phys. Chem. A*, 2021, **125**, 2021–2050.
40 T. M. Cardozo and M. A. C. Nascimento, *J. Chem. Phys.*, 2009, **130**, 104102.
41 F. Fantuzzi and M. A. C. Nascimento, *J. Chem. Theory Comput.*, 2014, **10**, 2322–2332.
42 F. Fantuzzi, D. W. O. de Sousa and M. A. C. Nascimento, *ChemistrySelect*, 2017, **2**, 604–619.

Downloaded from http://books.rsc.org/books/edited-volume/chapter-pdf/1851664/bk9781837676200-00271.pdf by University of Kent user on 28 January 2025

43 T. M. Cardozo, D. W. Oliveira De Sousa, F. Fantuzzi and M. A. C. Nascimento, in *Comprehensive Computational Chemistry*, Elsevier, 2024, pp. 552–588.
44 F. A. Bobrowicz and W. A. Goddard, in *Methods of Electronic Structure Theory*, ed. H. F. Schaefer, 1977, p. 108.
45 M. A. C. Nascimento, *Int. J. Quantum Chem.*, 2019, **119**, e25765.
46 M. A. C. Nascimento, *Molecules*, 2021, **26**, 4524.
47 L. T. Xu and T. H. Dunning, *J. Chem. Phys.*, 2022, **157**, 014107.
48 S. Shaik, D. Danovich and P. C. Hiberty, *J. Chem. Phys.*, 2022, **157**, 090901.
49 D. Hagebaum-Reignier, J. Racine and S. Humbel, *J. Chem. Phys.*, 2022, **156**, 204310.
50 W. Koch and M. C. Holthausen, *A chemist's guide to density functional theory*, Wiley-VCH, 2001.
51 R. G. Parr and W. Yang, *Density-functional theory of atoms and molecules*, Oxford University Press, New York, New York, 1989.
52 E. Engel and R. M. Dreizler, *Density Functional Theory: An Advanced Course*, Springer Berlin Heidelberg, Berlin, Heidelberg, 2011.
53 N. Mardirossian and M. Head-Gordon, *Mol. Phys.*, 2017, **115**, 2315–2372.
54 M. Bursch, J. Mewes, A. Hansen and S. Grimme, *Angew. Chem., Int. Ed.*, 2022, **61**, e202205735.
55 S. Grimme, J. Antony, S. Ehrlich and H. Krieg, *J. Chem. Phys.*, 2010, **132**, 154104.
56 S. Grimme, S. Ehrlich and L. Goerigk, *J. Comput. Chem.*, 2011, **32**, 1456–1465.
57 E. Caldeweyher, J.-M. Mewes, S. Ehlert and S. Grimme, *Phys. Chem. Chem. Phys.*, 2020, **22**, 8499–8512.
58 E. Livshits and R. Baer, *Phys. Chem. Chem. Phys.*, 2007, **9**, 2932.
59 J. P. Perdew and K. Schmidt, in *AIP Conference Proceedings*, AIP, 2001, vol. 577, pp. 1–20.
60 P. J. Hay and W. R. Wadt, *J. Chem. Phys.*, 1985, **82**, 299–310.
61 F. Weigend and R. Ahlrichs, *Phys. Chem. Chem. Phys.*, 2005, **7**, 3297.
62 E. van Lenthe, J. G. Snijders and E. J. Baerends, *J. Chem. Phys.*, 1996, **105**, 6505–6516.
63 E. van Lenthe, E. J. Baerends and J. G. Snijders, *J. Chem. Phys.*, 1994, **101**, 9783–9792.
64 E. van Lenthe, E. J. Baerends and J. G. Snijders, *J. Chem. Phys.*, 1993, **99**, 4597–4610.
65 B. A. Hess, *Phys. Rev. A: At., Mol., Opt. Phys.*, 1986, **33**, 3742–3748.
66 M. Douglas and N. M. Kroll, *Ann. Phys.*, 1974, **82**, 89–155.
67 A. T. B. Gilbert, N. A. Besley and P. M. W. Gill, *J. Phys. Chem. A*, 2008, **112**, 13164–13171.
68 V. Barone, S. Alessandrini, M. Biczysko, J. R. Cheeseman, D. C. Clary, A. B. McCoy, R. J. DiRisio, F. Neese, M. Melosso and C. Puzzarini, *Nat. Rev. Methods Primers*, 2021, **1**, 38.
69 R. McWeeny, *Methods of molecular quantum mechanics*, Academic Press, London, 2nd edn, 1989.
70 R. C. Hilborn, *Am. J. Phys.*, 1982, **50**, 982–986.
71 S. L. Li and D. G. Truhlar, *J. Chem. Theory Comput.*, 2017, **13**, 2823–2830.
72 T. J. Zuehlsdorff and C. M. Isborn, *Int. J. Quantum Chem.*, 2019, **119**, e25719.
73 E. Benassi, C. Cappelli, B. Carlotti and V. Barone, *Phys. Chem. Chem. Phys.*, 2014, **16**, 26963–26973.
74 J. Bednarska, R. Zaleśny, G. Tian, N. Murugan, H. Ågren and W. Bartkowiak, *Molecules*, 2017, **22**, 1643.
75 T. Petrenko and F. Neese, *J. Chem. Phys.*, 2007, **127**, 164319.

Downloaded from http://books.rsc.org/books/edited-volume/chapter-pdf/1851664/bk9781837676200-00271.pdf by University of Kent user on 28 January 2025

76 E. F. Petrusevich, M. H. E. Bousquet, B. Ośmiałowski, D. Jacquemin, J. M. Luis and R. Zaleśny, *J. Chem. Theory Comput.*, 2023, **19**, 2304–2315.
77 F. J. Avila Ferrer, J. Cerezo, J. Soto, R. Improta and F. Santoro, *Comput. Theor. Chem.*, 2014, **1040–1041**, 328–337.
78 P. P. Fehér, Á. Madarász and A. Stirling, *J. Chem. Theory Comput.*, 2021, **17**, 6340–6352.
79 S. Abou-Hatab, V. Carnevale and S. Matsika, *J. Chem. Phys.*, 2021, **154**, 064104.
80 S. Tsuru, B. Sharma, M. Nagasaka and C. Hättig, *J. Phys. Chem. A*, 2021, **125**, 7198–7206.
81 W. Arbelo-González, R. Crespo-Otero and M. Barbatti, *J. Chem. Theory Comput.*, 2016, **12**, 5037–5049.
82 R. Crespo-Otero and M. Barbatti, in *Marco Antonio Chaer Nascimento*, 2014, pp. 89–102.
83 M. Barbatti, *J. Chem. Theory Comput.*, 2020, **16**, 4849–4856.
84 M. Barbatti, A. J. A. Aquino and H. Lischka, *Phys. Chem. Chem. Phys.*, 2010, **12**, 4959.
85 L. E. de Sousa and P. de Silva, *J. Phys. Chem. A*, 2023, **127**, 8200–8208.
86 C. A. Ullrich, *Time-dependent density-functional theory: concepts and applications*, Oxford University Press, Oxford, 2012.
87 F. W. Byron and R. W. Fuller, *Mathematics of classical and quantum physics*, Dover, New York, 1992.
88 M. Nooijen and R. J. Bartlett, *J. Chem. Phys.*, 1997, **107**, 6812–6830.
89 J. Schirmer, *Phys. Rev. A: At., Mol., Opt. Phys.*, 1982, **26**, 2395–2416.
90 A. Dreuw, A. Papapostolou and A. L. Dempwolff, *J. Phys. Chem. A*, 2023, **127**, 6635–6646.
91 A. Yu. Sokolov, *J. Chem. Phys.*, 2018, **149**, 204113.
92 C. E. V. Moura and A. Yu. Sokolov, *J. Phys. Chem. A*, 2024, **128**, 5816–5831.
93 N. P. Gaba, C. E. V. de Moura, R. Majumder and A. Yu. Sokolov, *Phys. Chem. Chem. Phys.*, 2024, **26**, 15927–15938.
94 L. Serrano-Andrés, D. Roca-Sanjuán and G. Olaso-González, in *Photochemistry*, The Royal Society of Chemistry, 2010, pp. 10–36.
95 Y.-J. Liu, D. Roca-Sanjuán and R. Lindh, in *Photochemistry*, The Royal Society of Chemistry, 2012, pp. 42–72.
96 L. González, D. Escudero and L. Serrano-Andrés, *ChemPhysChem*, 2012, **13**, 28–51.
97 C. Daniel, *Coord. Chem. Rev.*, 2015, **282–283**, 19–32.
98 N. M. S. Almeida, R. G. McKinlay and M. J. Paterson, in *Computational Studies in Organometallic Chemistry. Structure and Bonding*, ed. S. A. Macgregor and O. Eisenstein, Springer, Cham, 2014, vol. 167, pp. 107–138.
99 J. P. Zobel and L. González, *JACS Au*, 2021, **1**, 1116–1140.
100 C. Latouche, D. Skouteris, F. Palazzetti and V. Barone, *J. Chem. Theory Comput.*, 2015, **11**, 3281–3289.
101 S. Paranthaman, J. Moon, J. Kim, D. E. Kim and T. K. Kim, *J. Phys. Chem. A*, 2016, **120**, 2128–2134.
102 C. Garino and L. Salassa, *Philos. Trans. R. Soc., A*, 2013, **371**, 20120134.
103 J. N. Harvey, *Annu. Rep. Prog. Chem., Sect. C: Phys. Chem.*, 2006, **102**, 203–226.
104 T. A. Niehaus, T. Hofbeck and H. Yersin, *RSC Adv.*, 2015, **5**, 63318–63329.
105 F. Maschietto, M. Campetella, J. Sanz García, C. Adamo and I. Ciofini, *J. Chem. Phys.*, 2021, **154**, 204102.
106 P. J. Costa, M. J. Calhorda, J. Bossert, C. Daniel and C. C. Romão, *Organometallics*, 2006, **25**, 5235–5241.
107 D. Escudero and L. González, *J. Chem. Theory Comput.*, 2012, **8**, 203–213.

Downloaded from http://books.rsc.org/books/edited-volume/chapter-pdf/1851664/bk9781837676200-00271.pdf by University of Kent user on 28 January 2025

108 A. Bousseksou, G. Molnár, L. Salmon and W. Nicolazzi, *Chem. Soc. Rev.*, 2011, **40**, 3313.
109 H. J. Shepherd, G. Molnár, W. Nicolazzi, L. Salmon and A. Bousseksou, *Eur. J. Inorg. Chem.*, 2013, **2013**, 653–661.
110 Q. M. Phung, M. Feldt, J. N. Harvey and K. Pierloot, *J. Chem. Theory Comput.*, 2018, **14**, 2446–2455.
111 M. Reimann and M. Kaupp, *J. Chem. Theory Comput.*, 2023, **19**, 97–108.
112 J. Cirera, M. Via-Nadal and E. Ruiz, *Inorg. Chem.*, 2018, **57**, 14097–14105.
113 M. Radoń, *Phys. Chem. Chem. Phys.*, 2019, **21**, 4854–4870.
114 B. J. Powell, *Coord. Chem. Rev.*, 2015, **295**, 46–79.
115 P. Kumar and D. Escudero, *Inorg. Chem.*, 2021, **60**, 17230–17240.
116 H. D. Ludowieg, M. Srebro-Hooper, J. Crassous and J. Autschbach, *ChemistryOpen*, 2022, **11**, e202200020.
117 M. Patra and G. Gasser, *ChemBioChem*, 2012, **13**, 1232–1252.
118 B. Bertrand, K. Passador, C. Goze, F. Denat, E. Bodio and M. Salmain, *Coord. Chem. Rev.*, 2018, **358**, 108–124.
119 M. Feldt and A. Brown, *J. Comput. Chem.*, 2021, **42**, 144–155.
120 M. R. Momeni and A. Brown, *J. Chem. Theory Comput.*, 2015, **11**, 2619–2632.
121 Í. A. O. Bozzi, L. A. Machado, E. B. T. Diogo, F. G. Delolo, L. O. F. Barros, G. A. P. Graça, M. H. Araujo, F. T. Martins, L. F. Pedrosa, L. C. da Luz, E. S. Moraes, F. S. Rodembusch, J. S. F. Guimarães, A. G. Oliveira, S. H. Röttger, D. B. Werz, C. P. Souza, F. Fantuzzi, J. Han, T. B. Marder, H. Braunschweig and E. N. da Silva Júnior, *Chem. – Eur. J.*, 2024, **30**, e202303883.
122 V. Postils, F. Ruipérez and D. Casanova, *J. Chem. Theory Comput.*, 2021, **17**, 5825–5838.
123 R. Berraud-Pache, F. Neese, G. Bistoni and R. Izsák, *J. Chem. Theory Comput.*, 2020, **16**, 564–575.
124 C. R. Brewer, O. M. Hawkins, N. C. Sheehan, J. D. Bullock, V. D. Kleiman, A. V. Walker and L. McElwee-White, *Organometallics*, 2019, **38**, 4363–4370.
125 C. R. Brewer, N. C. Sheehan, J. Herrera, A. V. Walker and L. McElwee-White, *Organometallics*, 2022, **41**, 761–775.
126 B. G. Salazar, C. R. Brewer, L. McElwee-White and A. V. Walker, *J. Vac. Sci. Technol., A*, 2022, **40**, 023404.
127 M. Zlatar, M. Allan and J. Fedor, *J. Phys. Chem. C*, 2016, **120**, 10667–10674.
128 S. Osella, *Nanomaterials*, 2021, **11**, 299.
129 K. R. Yang, G. W. Kyro and V. S. Batista, *Nat. Comput. Sci.*, 2023, **3**, 504–513.
130 M. Loipersberger, D. Z. Zee, J. A. Panetier, C. J. Chang, J. R. Long and M. Head-Gordon, *Inorg. Chem.*, 2020, **59**, 8146–8160.
131 D. Z. Zee, M. Nippe, A. E. King, C. J. Chang and J. R. Long, *Inorg. Chem.*, 2020, **59**, 5206–5217.
132 N. H. List, C. Curutchet, S. Knecht, B. Mennucci and J. Kongsted, *J. Chem. Theory Comput.*, 2013, **9**, 4928–4938.

Downloaded from http://books.rsc.org/books/edited-volume/chapter-pdf/1851664/bk9781837676200-00271.pdf by University of Kent user on 28 January 2025